

RESEARCH ARTICLE

Characterization of a novel pyruvate kinase from *Trichinella spiralis* and its participation in sugar metabolism, larval molting and development

Wen Wen Yue, Shu Wei Yan, Ru Zhang, Yong Kang Cheng, Ruo Dan Liu, Shao Rong Long, Xi Zhang, Zhong Quan Wang*, Jing Cui^{ID}*

Department of Parasitology, Medical College, Zhengzhou University, Zhengzhou, People's Republic of China

* wangzq@zzu.edu.cn (ZQW); cuij@zzu.edu.cn (JC)



Abstract

Background

Pyruvate kinase widely exists in many parasites and plays an important role in the energy production for the parasites. Pyruvate kinase might be a potential drug target for killing the parasites. The aim of the present study was to evaluate the biological characteristics and roles of *T. spiralis* pyruvate kinase M (TsPKM) in sugar metabolism, larval molting and development of *T. spiralis*.

Methodology/Principal findings

TsPKM has two functional domains of pyruvate kinase and the tertiary structure of TsPKM is tetramer which has the enzyme active site constituted by 8 amino-acid residues (Arg71, Asn73, Asp110, Phe241, Lys267, Glu269, Asp293 and Thr325). Recombinant TsPKM (rTsPKM) was expressed and purified. The rTsPKM had good immunogenicity. RT-PCR and Western blot showed that TsPKM was transcribed and expressed at various developmental stages in *T. spiralis* lifecycle. Immunofluorescence test showed that TsPKM was principally located in the cuticle, muscle, stichosome, intestine and the intrauterine embryos of female adults. rTsPKM catalyzed the reaction of phosphoenolpyruvate (PEP) and adenosine diphosphate (ADP) to produce pyruvic acid and adenosine triphosphate (ATP). TsPKM played an important role in the metabolism and energy production of *T. spiralis*. After silencing of TsPKM gene by specific dsRNA-TsPKM2, protein expression and enzyme activity of TsPKM decreased by 50.91 and 26.06%, respectively. After treatment with RNAi, natural TsPKM enzyme activity, larval molting, sugar metabolism, growth and development of *T. spiralis* were significantly reduced.

Conclusions

TsPKM participates in the larval molting, sugar metabolism, growth and development of *T. spiralis* and it might be a candidate target of therapeutic drug of trichinellosis.

OPEN ACCESS

Citation: Yue WW, Yan SW, Zhang R, Cheng YK, Liu RD, Long SR, et al. (2022) Characterization of a novel pyruvate kinase from *Trichinella spiralis* and its participation in sugar metabolism, larval molting and development. PLoS Negl Trop Dis 16(10): e0010881. <https://doi.org/10.1371/journal.pntd.0010881>

Editor: Krystyna Cwiklinski, University of Liverpool, UNITED KINGDOM

Received: May 24, 2022

Accepted: October 10, 2022

Published: October 31, 2022

Copyright: © 2022 Yue et al. This is an open access article distributed under the terms of the [Creative Commons Attribution License](https://creativecommons.org/licenses/by/4.0/), which permits unrestricted use, distribution, and reproduction in any medium, provided the original author and source are credited.

Data Availability Statement: All relevant data are within the manuscript and its [Supporting Information](#) files.

Funding: This study was supported by grants of the National Natural Science Foundation of China (No. 81871673, 82172300) awarded to JC. The funders had no role in the study design, data collection and analysis, decision to publish, or preparation of the manuscript.

Competing interests: The authors have declared that no competing interests exist.

Author summary

Pyruvate kinases belong to transferases and can transfer the high-energy phosphate bond of phosphoenolpyruvate (PEP) to adenosine diphosphate (ADP) to produce pyruvic acid and adenosine triphosphate (ATP). Pyruvate kinases play a significant biological role in the parasite survival in hosts. Our results revealed that TsPKM was expressed at various *T. spiralis* developmental stages, and principally located in the cuticle, stichosome, intestine and the intrauterine embryos of female adults. rTsPKM catalyzed the reaction of phosphoenolpyruvate (PEP) and adenosine diphosphate (ADP) to produce pyruvic acid and adenosine triphosphate (ATP). TsPKM played an important role in the metabolism and energy production of *T. spiralis*. Protein expression and enzyme activity of TsPKM were decreased by 50.91 and 26.06% respectively through silencing of TsPKM gene using specific dsRNA-TsPKM2. After treatment with RNAi and inhibitor tannin, natural TsPKM activity, larval molting, sugar metabolism, growth and development of *T. spiralis* were obviously inhibited. Our results showed that TsPKM participates in *T. spiralis* molting, sugar metabolism and development, and it might be a candidate target for anti-*Trichinella* drugs.

Introduction

Trichinella spiralis is a tissue-parasiting nematode of the genus *Trichinella* that causes trichinellosis. Trichinellosis is a zoonotic parasitic disease caused by eating raw or semi-raw meat containing the encapsulated infective muscle larvae (ML), which is widely prevalent all over the world [1]. From 2009 to 2020, there were 8 outbreaks of human trichinellosis in China, which consisted of 479 cases and 2 deaths [2]. Pork is the predominant source of *T. spiralis* infection in humans. *Trichinella* infection is not only an important public health problem but also a tremendous threat to meat food safety [3–5].

After being ingested, the encapsulated ML in infected meat are released from their capsules under the help of gastric digestive enzymes and activated into intestinal infectious larvae (IIL) by bile, the IIL invade into enteral epithelium and undergo molting four times to develop into adult worms (AW) [6,7]. The female AW produce newborn larvae (NBL) that circulates via the lymph to bloodstream and invade the skeletal muscles to develop into the encapsulated ML for completing their lifecycle [8]. *T. spiralis* mainly obtains various energy required for its survival through glucose metabolism, and generally has a complete citric acid cycle [9]. Hexokinase, phosphofructokinase-1 and pyruvate kinase are the three key enzymes in glycolysis pathway. Pyruvate kinase belongs to transferases, and it can catalyze the reaction of phosphoenolpyruvate (PEP) and adenosine diphosphate (ADP) to produce pyruvic acid and adenosine triphosphate (ATP). ATP produced by catalysis provides energy for the organisms. Pyruvic acid participates in the subsequent aerobic and anaerobic oxidation to provide energy for the life activities of the organisms. At the same time, it completes the conversion of sugar, fat and amino acids under the action of acetyl coenzyme A and citric acid cycle [10]. Glycolysis is a common pathway of anaerobic and aerobic oxidation of sugar, which is from the phosphorylation of glucose to the final production of Pyruvic acid. All factors that affect glycolysis also affect the anaerobic and aerobic oxidation of sugar, thus affecting the utilization of glucose, the synthesis of ATP and the conversion of three nutrients. Therefore, pyruvate kinase plays an important role in cell metabolism.

Pyruvate kinase widely exists in some free-living nematode and parasites, such as *Caenorhabditis elegans* [11], *Schistosoma japonicum* [12], cestode [13], *Giardia lamblia* [14], *Plasmodium* [15], *Toxoplasma gondii* [16] and *Cryptosporidium* [17]. It plays an important role in the energy production for the parasites and the nutrient conversion, and then affects the growth, development and reproduction of parasites. Due to the important role of pyruvate kinase in cell metabolism, the energy of parasites can be exhausted by inhibiting or knocking out the expression of pyruvate kinase gene, which can lead to parasite death. Therefore, pyruvate kinase is a potential drug target for killing the parasites.

In this study, a novel *T. spiralis* pyruvate kinase M (TsPKM, GenBank: KRY30732.1) was acquired from *T. spiralis* draft genome [18]. In mammals, pyruvate kinase was divided into three different subtypes, namely PKL, PKR and PKM (PKM1 and PKM2). PKL is mainly expressed in liver, kidney and intestine; PKR is expressed in red blood cells, and PKM is principally expressed in tissues with high energy metabolism and rapidly proliferating cells [19]. The pyruvate kinase from *T. spiralis* is assigned to the PKM subtype. The aim of the present study was to evaluate the biological characteristics and roles of TsPKM in sugar metabolism, larval molting and development of *T. spiralis*.

Materials and methods

Ethics statement

This study was performed in the light of National Guidelines for Experimental Animal Welfare (Minister of Science and Technology, People's Republic of China, 2006). All animal experiments in the current research were approved by the Life Science Ethics Committee of Zhengzhou University (No. SCXK 2020–0004).

Parasites, cells and experimental animals

The species of *Trichinella spiralis* (ISS534) was collected from a naturally infected domestic pig in central China [20], and passaged in BALB/c mice in our laboratory. Intestinal epithelium cells (IECs) were isolated from small intestine of normal fetal mice [21,22]. Female BALB/c mice aged 4–6 weeks were purchased from Henan Provincial Experimental Animal Center.

Worm collection and protein preparation

The ML were collected by artificial digestion of *T. spiralis*-infected mouse muscles at 42 days post infection (dpi) [23]. The IIL were recovered from the intestine of infected mice at 6 hours post infection (hpi) [24,25]. The AW at 3 and 6 dpi were also collected from infected murine small intestine [26]. The adult females at 6 dpi were cultured in RPMI-1640 with 10% fetal bovine serum (FBS; Gibco) at 37°C in 5% CO₂ for 24 h, and the NBL were harvested as previously described [27]. Worm soluble proteins of various stage worms (ML, IIL, AW and NBL), excretion and secretion (ES) proteins from ML, IIL and AW were prepared as described previously [28,29]. Briefly, various *T. spiralis* stages (ML, IIL and AW) were washed using sterile saline, cultured in RPMI-1640 medium (5000 worms/ml) at 37°C, 5% CO₂ for 18 h. The culture medium containing ES proteins was filtered by a 0.22 μm membrane, and concentrated using an ultrafiltration tube. The concentration of ES proteins was assayed by a Coomassie brilliant blue G-250 method [26].

Bioinformatics analysis of TsPKM

The full-length cDNA sequence of TsPKM gene was retrieved from GenBank (GenBank: KRY30732.1) [30]. The physicochemical properties and biological characteristics were

analyzed through the online bioinformatics website. Multiple sequence alignment of the amino acid sequence of pyruvate kinase among different species of the genus *Trichinella* was compared by Cluster Omega [31,32]. The GenBank accession numbers of pyruvate kinase from other *Trichinella* species and organisms were as follows: *Trichinella* T8 (KRZ85571.1), *Trichinella* T6 (KRX84774.1), *T. murrelli* (KRX42370.1), *T. nativa* (OUC39704.1), *T. britovi* (KRY55915.1), *T. patagoniensis* (KRY12085.1), *T. nelsoni* (KRX15479.1), *T. pseudospiralis* (KRX90766.1), *T. papuae* (KRZ80248.1), *T. zimbabwensis* (KRZ04871.1), *Homo sapiens* (AAA60104.1) and *Mus musculus* (BAA23642.1). The phylogenetic tree was constructed using MEGA 7.0 on the basis of the Neighbor-joining (NJ) method as described before [33,34].

Cloning and expression of rTsPKM and preparation of anti-rTsPKM serum

Total RNA was extracted from the ML using Trizol (Invitrogen, USA), reversely transcribed into the cDNA and used as a template to amplify the TsPKM gene. *Bam*HI and *Pst*I (**Bold**) were selected as restriction sites to design TsPKM-specific primers (5'-CGCGGATCCATGTCCGAAAAGCAAAGTCAGAAGA-3', 5'-AACTGCAGTCATGGTCTTGAATTAGAGGTTTCG-3') [35]. The full length TsPKM cDNA sequence was amplified by PCR. The PCR products were cloned into the expression vector pQE-80L with a His-tag at N-terminus (Novagen, USA), and recombinant pQE-80L/TsPKM was introduced into *E. coli* BL21 (Novagen). The expression of rTsPKM was induced at 25°C for 23 h using 0.2 mM IPTG [36], rTsPKM was purified by nickel column affinity chromatography (Sangon Biotech, Shanghai, China) [37]. Expression of rTsPKM protein was analyzed by SDS-PAGE and Western blotting as described before [38].

Ten mice were immunized subcutaneously with 20 µg rTsPKM mixed with complete Freund's adjuvant. Boost immunization was administered three times with 20 µg rTsPKM mixed with incomplete Freund's adjuvant at a 2-week interval [39]. Two weeks after the last immunization, tail blood of immunized mice was collected to isolate anti-rTsPKM immune sera, the IgG antibody titer of anti-rTsPKM serum was measured by ELISA [40,41].

SDS-PAGE and Western blotting analysis

Soluble worm somatic crude and ES proteins of diverse *T. spiralis* phases, and purified rTsPKM were separated on 10% SDS-PAGE [24,42]. The proteins were transferred onto nitrocellulose (NC) membrane (Millipore, USA) in the semi-dry transfer cell (Bio-Rad, USA) [43]. The membrane was blocked with 5% skimmed milk in Tris-buffered saline containing 0.05% Tween (TBST) at 37°C for 2 h, and cut into strips. The strips were probed by various sera (1:100; anti-rTsPKM serum, infection serum and pre-immune serum) at 37°C for 2 h. After washes with TBST, the strips were incubated at 37°C for 1 h with HRP-anti-mouse IgG conjugate (1:10000; Southern Biotech, USA). After being washed again, the strips were colored using 3, 3'-diaminobenzidine tetrahydrochloride (DAB; Sigma-Aldrich) or an enhanced chemiluminescent kit (ECL, Solarbio, China) [44,45].

RT-PCR analysis of TsPKM transcription in different *T. spiralis* phases

Total RNAs from diverse *T. spiralis* stages (ML, IIL, 3 d AW and NBL) were isolated using Trizol (Invitrogen, USA) [46,47]. RT-PCR was performed to evaluate the TsPKM mRNA expression in diverse *T. spiralis* stages as previously described [48]. A *T. spiralis* housekeeping gene GAPDH (GenBank: AF452239) was also amplified and used as an internal control [49,50]. Each experiment had three replicates.

Immunofluorescence test (IFT)

The fresh whole worms of different *Trichinella spiralis* stages (ML, IIL, 3 d AW and NBL) were fixed with 4% paraformaldehyde for 30 min and embedded in paraffin and cut into a 2- μ m thick cross-section with a microtome. Expression and worm tissue localization of natural TsPKM in diverse worm stages were investigated using the IFT technique as reported before [43,51]. Briefly, the whole worms and cross-sections were first blocked with 5% goat serum at 37°C for 2 h, and then incubated at 37°C for 2 h with various sera (1: 10 dilutions of anti-rTsPKM serum, infection serum and normal serum). After washes with PBS, the worms and cross-sections were incubated with FITC-conjugated anti-mouse IgG (1:100; Abways, Shanghai, China). After washes again, they were observed under fluorescent microscopy (Olympus, Tokyo, Japan) [52,53].

Enzyme activity analysis of rTsPKM

The enzyme activity of rTsPKM was assayed by using 2,4-dinitrophenylhydrazine method. The reaction mixture composition and reaction conditions are as follows. rTsPKM (8 μ l) was first added into matrix solution (32 μ l; 2.5 mM PEP, 1.25 mM ADP, pH 8.0 Tris-HCl), and incubated at 37°C for 10 min. The reaction was terminated with incubation of 80 μ l of reaction stop solution (0.0625 g 2,4-dinitrophenylhydrazine, 25 ml of 10 mol/L HCl, 250 ml distilled water) at 37°C for 10 min. Coloration was developed with 8 μ l of coloration solution (730.6 mg EDTA, 100 ml distilled water, 2.5 mol/L NaOH 400 ml). Finally, a microplate reader was used to measure the absorbance at 510 nm. The *in vitro* optimum catalytic conditions of rTsPKM were determined by changing the concentration of rTsPKM, reaction temperature and pH of buffer solution [54]. In order to verify whether rTsPKM enzymatic activity is metal ion-dependent, seven common auxiliary metal ions (Fe^{2+} , Mn^{2+} , Ca^{2+} , Co^{2+} , Ni^{2+} , Cu^{2+} and Zn^{2+}) were added into the reaction system at the same concentration (0.3 mM) to analyze their effect on rTsPKM activity [49,55]. Previous studies showed that ethyl pyruvate had little side effects on humans and was easy to penetrate the blood brain barrier [56]. Therefore, ethyl pyruvate was also used as the enzyme inhibitor of TsPKM in the current study. Different concentrations of inhibitors (tannin, ethyl pyruvate) and common protease inhibitors 1,10-phenanthroline (1 mM), E64 (5 μ M), EDTA (10 mM) and PMSF (1 mM) were added to the reaction system to determine the effects of different inhibitors on rTsPKM enzyme activity [57]. Under the optimum catalytic conditions of rTsPKM enzyme activity, the corresponding enzyme kinetic parameters were determined by detecting the reaction of ADP with various concentrations of PEP, and the reaction of PEP with different concentrations of ADP [28].

Suppression of inhibitors on native TsPKM activity in worm somatic proteins

Total of 2000 ML were first incubated with at 37°C for 2 hours with various doses of tannin (25, 50, 75 and 100 μ M) or ethyl pyruvate (10, 20, 30, 40 mM) [56,58]. After being washed with PBS for 3 times, the larval soluble proteins were prepared [59]. The enzyme activity of native TsPKM in ML somatic proteins was measured by 2,4-dinitrophenylhydrazine method.

RNA interference (RNAi)

According to the cDNA sequence of TsPKM, three pairs of TsPKM-specific primers containing T7 promoter and enhancer were designed (5'-GATCACTAATACGACTCACT ATAGG GATGTCCGAAAAGCAAAGT-3', 5'-GATCACTAATACGACTCACTATAGGG CGTCA CCCTCACAGCGCTGTT-3'. 5'-GATCACTAATACGACTCACTATAGGGGATA

CCAAAGGGCCCCGAAAT-3', 5'-GATCACTAATACGACTCACTATAGGGTTCGATTTTGGCCACA-3'. 5'-GATCACTAATACGACTCACTATAGGGGTCAATTTGCCAGACTGT-3', 5'-GATCACTAATACGACTCACTATAGGGGTCTGCACCGTCCAGTAC-3') [27,60]. Green fluorescent protein (GFP) was selected as the control, and its primers were as follows: 5'-GATCACTAATACGACTCACTATAGGGTCTGTCGAGCTGGACGG-3', 5'-GATCACTAATACGACTCACTATAGGGCGCTTCTCGTTGGGGTCTTTG-3'. The dsRNA-TsPKM and dsRNA-GFP were transfected into the ML by electroporation (200 V 25 μ F 200 Ω) and cultured in RPMI-1640 for 3 days [61]. Transcription and expression levels of TsPKM gene in the ML were assessed by qPCR and Western blotting as described previously [62,63].

Effects of RNAi on the *in vitro* larval glycometabolism

Total 2000 ML were transfected with 60 ng/ μ l dsRNA-TsPKM2, dsRNA-GFP and PBS, respectively, and cultured for 3 days. Besides, 2000 ML were treated with 100 μ M tannin for 2 hours. Larval ATP contents from different groups were measured by ATP assay kit (Sangon Biotech, Shanghai, China). Moreover, the glycogen distribution in worm tissues was observed on larval sections using periodic acid-schiff stain (PAS; Baso, Zhuhai, China) [33,64]. The distribution of lipid droplets in whole intact ML was examined using oil red O staining [65]. Furthermore, the larval soluble somatic proteins were prepared, and total sugar and lipid content in larval soluble proteins was measured by anthrone-sulfuric method and acetylacetone method, respectively [66,67].

The *in vitro* larval molting test

The IIL are divided into four stages according to the molting time; include intestinal infective L₁ larvae (IIL1, 0.9 h after infection), L₂ larvae (10–14 h), L₃ larvae (15–22 h) and L₄ larvae (23–30 h) [62]. To assess the suppressive role of dsRNA-TsPKM and tannin on the larval molting, the *in vitro* invasion of mouse intestinal epithelial cells (IEC) was performed as previously described [42,68]. Briefly, ML was first activated into IIL1 using 5% swine bile at 37°C for 2 h. After washes with saline solution, the IIL larvae were treated by dsRNA-TsPKM or tannin, respectively. After treatment, fifty IIL were added to the semi-solid medium (DMEM+1.75% agarose) on an IEC monolayer and cultured in 37°C 5% CO₂ for 3 days [69]. Each group had triplicates. The larval molting was observed and counted under a light microscope [45].

Effects of RNAi on the *in vivo* larval development and glycometabolism

In order to further verify the TsPKM role in glycometabolism and development in *T. spiralis* life cycle, 100 mice were randomly divided into 5 groups (20 animals per group). Each mouse was orally with 500 ML treated with 60 ng/ μ l dsRNA-TsPKM2, dsRNA-GFP, PBS, tannin, or saline. All infected mice were euthanized at 24 h and 3 dpi, 24 h IIL (L₄ larvae) and 3 d AW were recovered and numbered from small intestine of infected mice as reported before [70,71]. The morphology, worm length from various groups of infected mice were observed and measured under microscopy [72]. Native TsPKM enzyme activity, sugar and lipid content of various stage worms from infected mice were also ascertained as before.

Statistical analysis

The data of this study were analyzed by SPSS 21.0 software and shown as arithmetic mean \pm SD (standard deviation). One-way ANOVA and Student's t test were used to analyze the difference in relative TsPKM mRNA transcription, protein expression, enzyme activity, larval glycolipid content, worm burdens and length. The differences of larval molting rate

among various groups were analyzed using Chi-square test. Statistical difference level was $P < 0.05$.

Results

Bioinformatics analysis of TsPKM

The complete cDNA sequence of TsPKM has a full length of 1629 bp and encodes 542 amino acids. The predicted molecular weight is 58.48 kDa and pI is 7.16. The TsPKM has obvious hydrophilicity at the N-terminus, and doesn't have transmembrane region and signal peptide. The amino acid sequences of the TsPKM had an identity of 98.71, 98.71, 98.53, 98.52, 98.34, 98.34 and 97.79% with pyruvate kinase of the 7 encapsulated *Trichinella* species/genotypes (*T. nativa*, *T. patagoniensis*, *T. murrelli*, *Trichinella* T8, *T. nelsoni*, *T. britovi*, and *Trichinella* T6), and it had an identity of 88.89, 88.21 and 88.21% with pyruvate kinase from 3 non-encapsulated *Trichinella* species (*T. pseudospiralis*, *T. papuae* and *T. zimbabwensis*) (Fig 1). TsPKM belonged to transferases. It had two functional domains of pyruvate kinase, and secondary structure had 25 α -helices, 32 β -strand, 18 β -turns, and 15 irregular coils. The tertiary structure analysis of TsPKM showed that the enzyme active site of TsPKM was constituted by 8 amino-acid residues (Arg71, Asn73, Asp110, Phe241, Lys267, Glu269, Asp293 and Thr325) (Fig 2A). The enzyme active site of TsPKM was highly conserved in different species of the genus *Trichinella* and also is the binding site of the metal ions (K^+ and Mg^{2+}) and substrate. The phylogenetic tree revealed that a monophyletic group of the genus *Trichinella* was well supported. Within the genus *Trichinella*, two clear clades were shown: one was the clade of 8 encapsulated species/genotypes (*T. spiralis*, *T. nativa*, *T. patagoniensis*, *T. murrelli*, *Trichinella* T8, *T. nelsoni*,

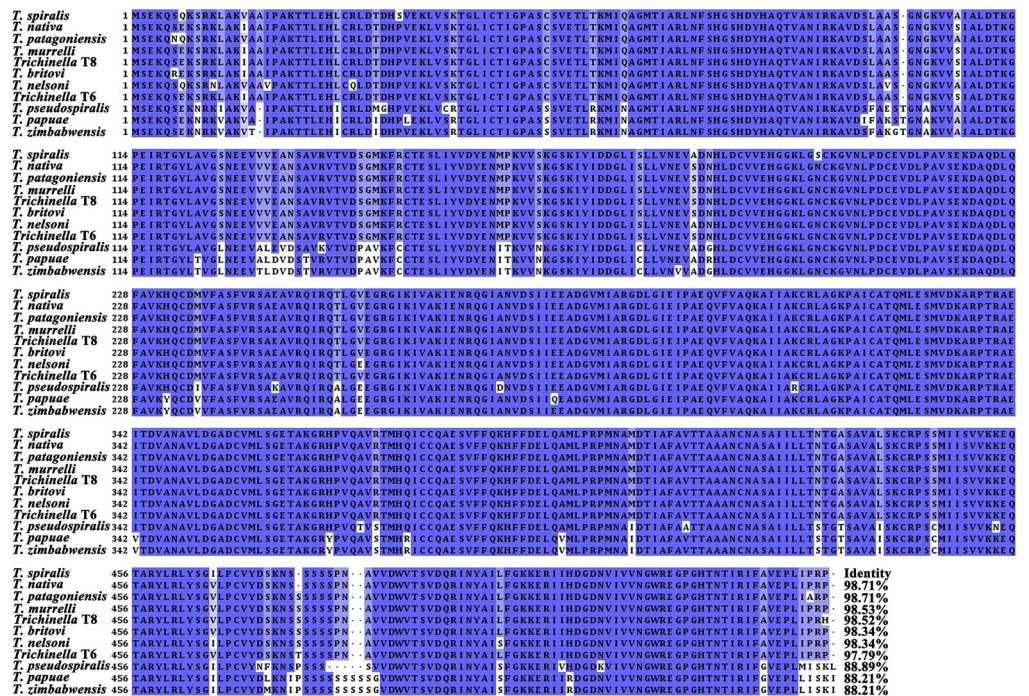


Fig 1. Multi sequence alignment of pyruvate kinase of different species/genotypes of *Trichinella*. According to the analysis of Cluster Omega, the same amino acids are marked in blue and conservative substitution of amino acid residues are marked in light blue. The pyruvate kinase genes of different species/genotypes of *Trichinella* have a high homology. The number at the end of each sequence represents the percentage of identity with TsPKM.

<https://doi.org/10.1371/journal.pntd.0010881.g001>

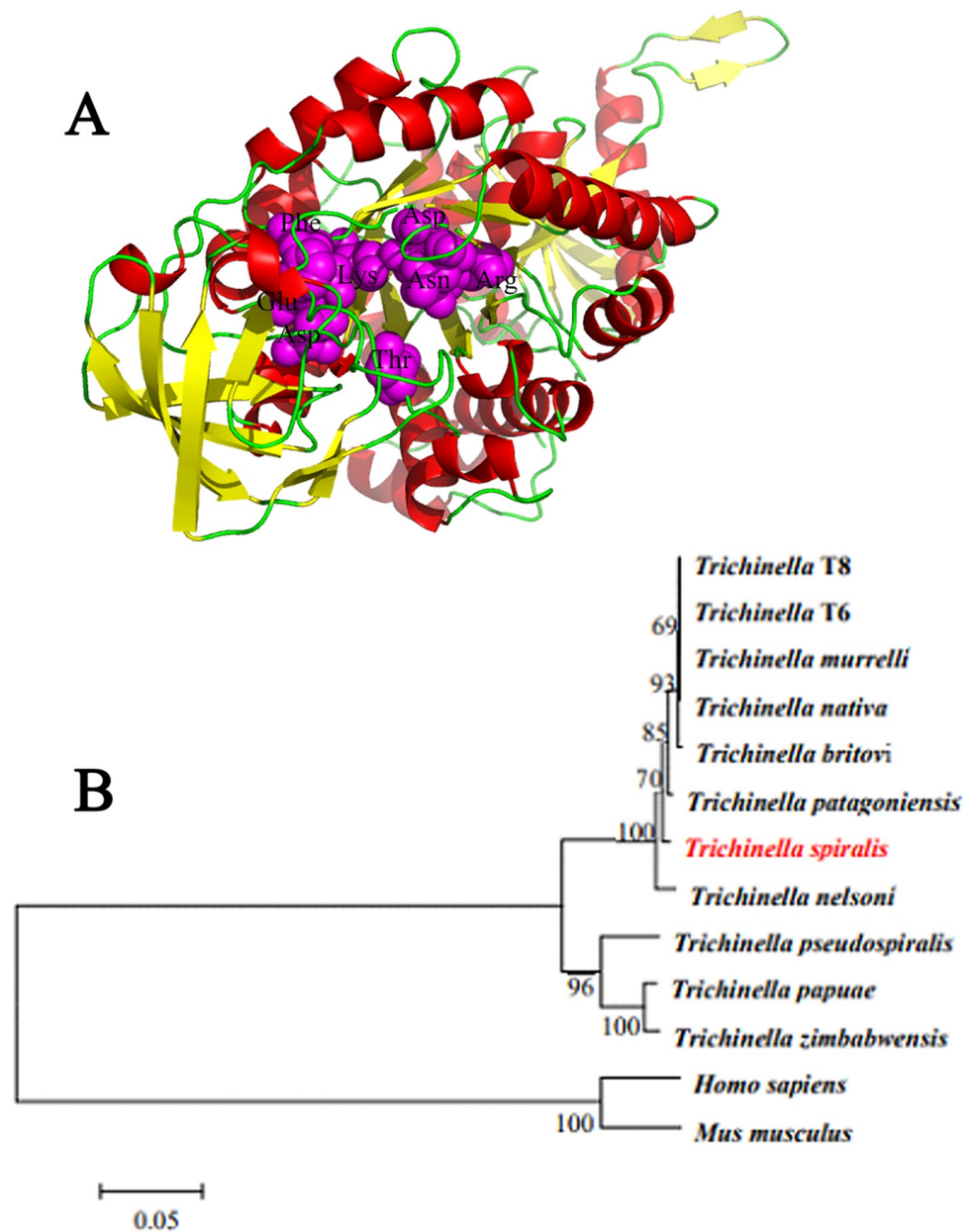


Fig 2. Tertiary structure prediction of TsPKM and evolutionary tree construction of pyruvate kinase of 13 organisms. **A:** Tertiary structure prediction of TsPKM. Eight amino-acid residues (Arg, Asn, Asp, Phe, Lys, Glu, Asp and Thr) constitute the enzyme active site signed as purple. **B:** TsPKM in the evolutionary tree of *Trichinella*, human and mouse. The evolutionary tree of pyruvate kinase of 11 different species/genotypes of the genus *Trichinella* was constructed by neighbor-joining (NJ) method. The encapsulated and non-encapsulated *Trichinella* was localized in two different evolutionary clades of *Trichinella*.

<https://doi.org/10.1371/journal.pntd.0010881.g002>

T. britovi, and *Trichinella* T6), and the other was the clade of three non-encapsulated species (*T. pseudospiralis*, *T. papuae* and *T. zimbabwensis*) (Fig 2B).

Expression and antigenic identification of rTsPKM

The SDS-PAGE results revealed that the molecular weight (MW) of the fusion protein expressed by the BL21 bacteria carrying pQE-80L/TsPKM was 58.48 kDa, which was

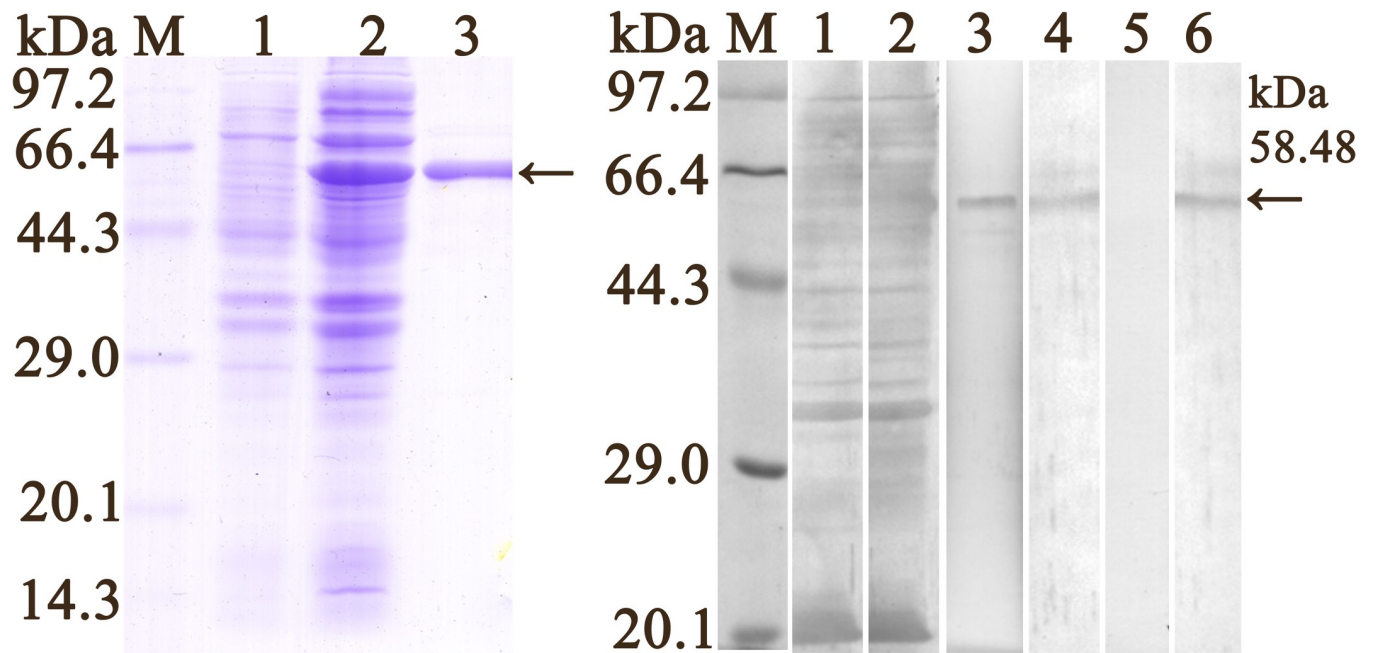


Fig 3. Expression and identification of rTsPKM. **A:** SDS-PAGE analysis of the rTsPKM. Lane M: Protein marker; Lane 1: lysate of recombinant *E. coli* incorporating pQE-80L/TsPKM prior to induction; Lane 2: lysate of recombinant *E. coli* incorporating pQE-80L/TsPKM after induction; Lane 3: purified rTsPKM. **B:** Western blotting analysis of rTsPKM antigenicity. Lane M: Protein marker; Lane 1: lysates of pQE-80L/TsPKM prior to induction were not recognized by infection serum. Lane 2: lysates of pQE-80L/TsPKM after induction were recognized by infection serum. The purified rTsPKM was recognized by anti-rTsPKM serum (lane 3), infection serum (lane 4) and anti-His tag McAb (lane 6), but not by normal serum (lane 5).

<https://doi.org/10.1371/journal.pntd.0010881.g003>

consistent with the predicted MW of the TsPKM protein (Fig 3A). In order to evaluate the humoral immune response induced by rTsPKM immunization, the titer of anti-rTsPKM IgG at two weeks after final immunization was detected by ELISA. The results showed that the IgG titer of anti-rTsPKM antibodies reached $1:10^5$ after four immunizations, indicating that rTsPKM had a good antigenicity. Western blotting analysis showed that rTsPKM was recognized by anti-rTsPKM serum, infection serum and anti-his tag monoclonal antibody (McAb) (Fig 3B), but not by pre-immune normal serum.

Transcription and expression of TsPKM in diverse *T. spiralis* stages

RT-PCR results revealed that TsPKM gene was transcribed in all various *T. spiralis* developmental stage (ML, IIL, 3 d AW and NBL), and the housekeeping gene GAPDH also generated an expected size (570 bp) in all stages of *T. spiralis* lifecycle (Fig 4A). On Western blotting analysis, native TsPKM in somatic crude proteins of various worm phases (ML, IIL, 3 d AW and NBL) was identified by anti-rTsPKM serum (Fig 4B and 4C), and the native TsPKM in ES proteins of various phases (ML, IIL and 6 d AW) was also detected by anti-rTsPKM serum (Fig 4D and 4E), indicating that TsPKM was transcribed and expressed at various developmental stages in *T. spiralis* lifecycle, and it was a somatic and secretory protein.

Expression and tissue localization of native TsPKM in various *T. spiralis* stages

The results of IFT with whole parasites revealed that bright green fluorescence was observed on the out surface of the cuticle of ML, IIL, 3 d AW and NBL using anti-rTsPKM serum and infection serum, but not by normal serum (Fig 5). The results of IFT with worm cross-sections

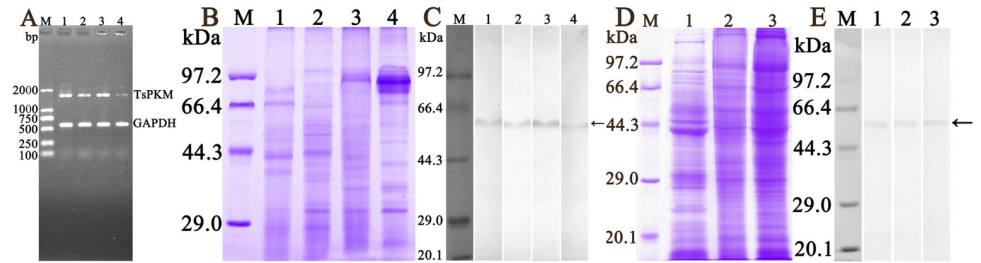


Fig 4. Transcription and expression of TsPKM in different stages of *Trichinella spiralis*. **A:** RT-PCR analysis of TsPKM transcription in diverse stages. Lane M: DNA marker; Lane 1: ML. Lane 2: 6 h IIL. Lane 3: 3 d AW. Lane 4: NBL. **B:** SDS-PAGE analysis of crude proteins of diverse worm stages. Lane M: protein marker. Lane 1: ML soluble protein. Lane 2: IIL soluble protein. Lane 3: 3 d AW soluble protein. Lane 4: NBL soluble protein. **C:** Western blot analysis of crude proteins of diverse worm stages of ML (lane 1), IIL (lane 2), 3 d AW (lane 3) and NBL (lane 4) identified using anti-rTsPKM serum. **D:** SDS-PAGE analysis of ES proteins of ML (lane 1), IIL (lane 2) and 6 d AW (lane 3), Lane M: protein marker. **E:** Western blot analysis of ES proteins of ML (lane 1), IIL (lane 2) and 6 d AW (lane 3) recognized by anti-rTsPKM serum. The recognized native TsPKM with about 58.5 kDa were indicated with arrows.

<https://doi.org/10.1371/journal.pntd.0010881.g004>

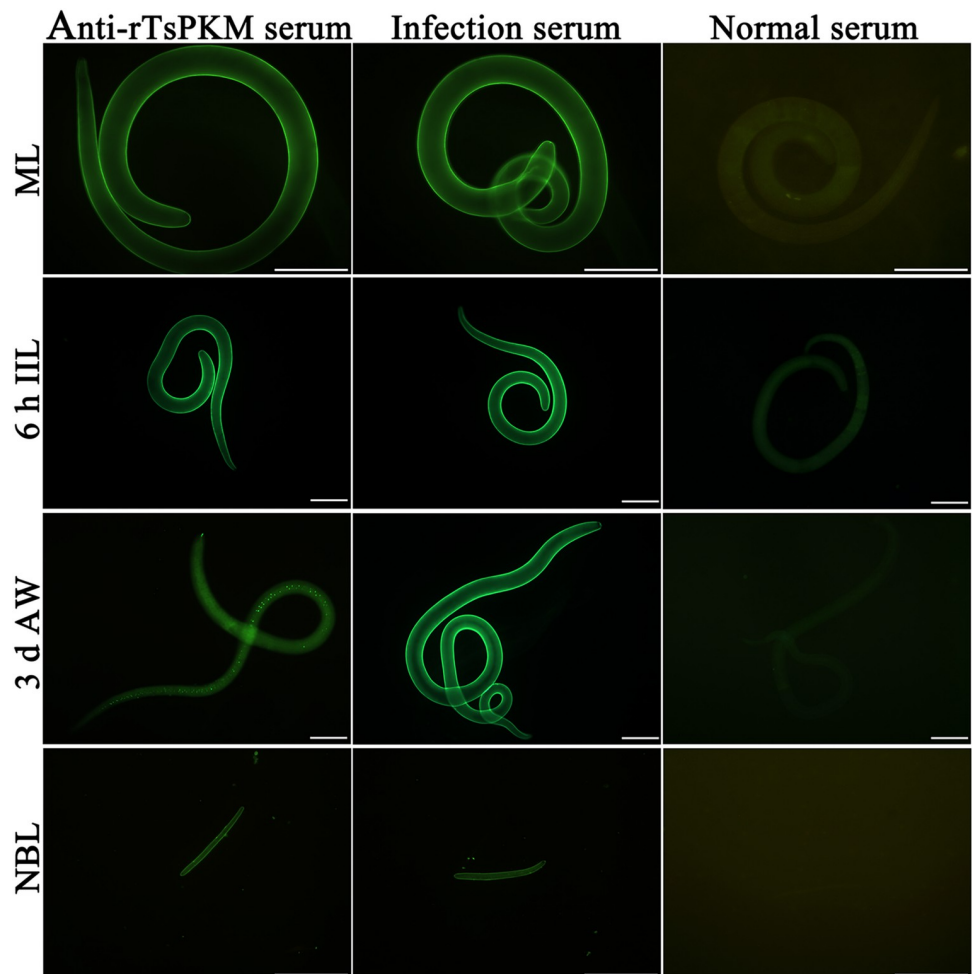


Fig 5. Expression of TsPKM at the cuticle of various *T. spiralis* stages by IFT. The whole intact worms were probed by anti-rTsPKM serum, and immune fluorescence staining was observed at the epicuticle of ML, IIL, NBL and the intestine of 3 d AW. But pre-immune normal serum did not recognize any worm components of the nematode. Scale bars: 100 μ m.

<https://doi.org/10.1371/journal.pntd.0010881.g005>

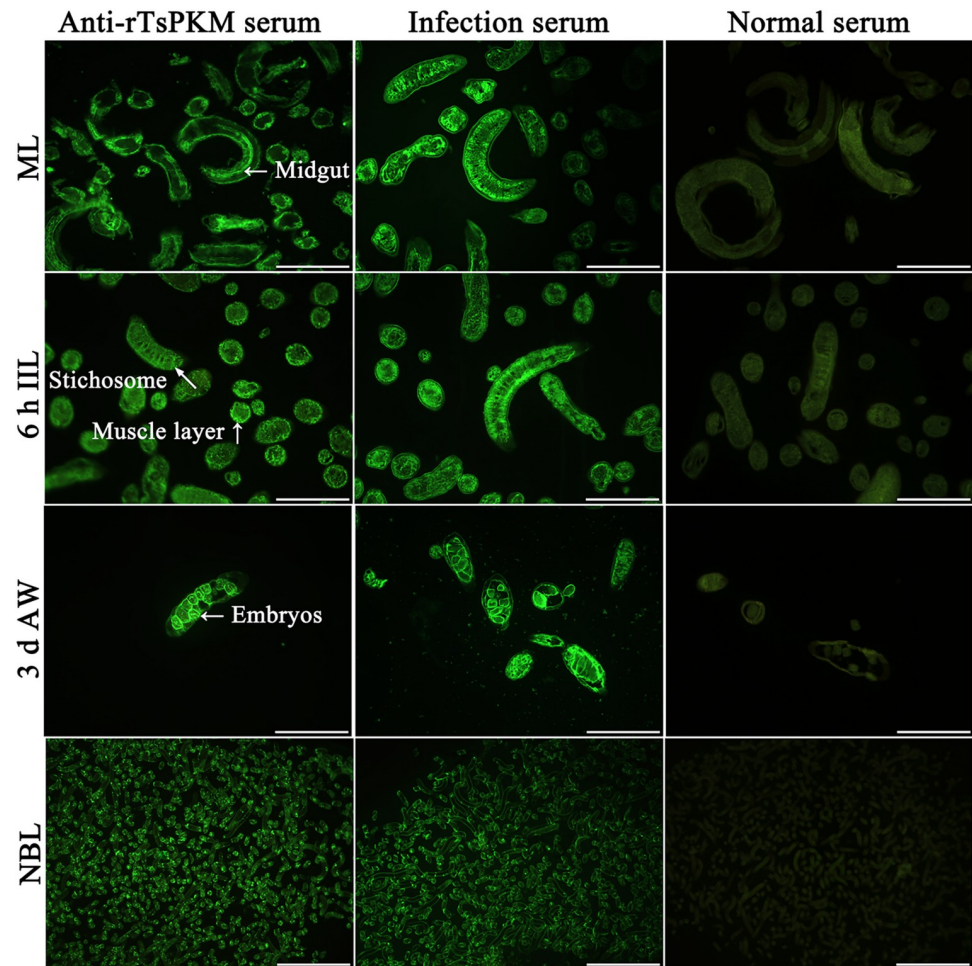


Fig 6. Immunolocalization of TsPKM in worm cross-sections of diverse *T. spiralis* stages by IFT with anti-rTsPKM serum. Green fluorescence staining was observed at cuticle, muscle, midgut, stichosome, and female intrauterine embryos. No immunostaining in worm cross-sections was observed by normal serum as a negative control. Scale-bars: 100 μm .

<https://doi.org/10.1371/journal.pntd.0010881.g006>

showed that immunostaining was primarily localized in the cuticle, muscle, stichosome, midgut and intrauterine embryos of the female adults (Fig 6).

Enzymatic activity of rTsPKM

The enzymatic activity of rTsPKM gradually increased with elevating rTsPKM concentration, and stabilized at a concentration of 10 ng/ μl (Fig 7A). The optimum temperature of rTsPKM for catalyzing the substrate reaction is 37°C, and the optimum buffer pH is 8.0 (Fig 7B and 7C). Metal ions K^+ and Mg^{2+} enhanced the enzyme activity of rTsPKM whereas Ni^{2+} , Fe^{2+} , Co^{2+} , Ca^{2+} , Mn^{2+} , Zn^{2+} and Cu^{2+} inhibited the enzyme activity of rTsPKM (Fig 7D). Tannin, ethyl pyruvate, EDTA and 1.10-Phe have obvious inhibitory effects on rTsPKM activity and tannin has the strongest inhibitory effect on rTsPKM activity (Fig 7E). The inhibitory effect of EDTA and 1.10-Phe is because the pyruvate kinase enzyme activity is metal dependent. The suppressive role of tannin ($r = 0.933$, $P < 0.0001$) and ethyl pyruvate ($r = 0.989$, $P < 0.0001$) on rTsPKM activity is dose-dependent (Fig 7F and 7G). The reaction conforms to the simple Michaelise-Menten kinetics (Fig 7H). The kinetic parameter V_{max} of PEP is 0.9469 mM/min

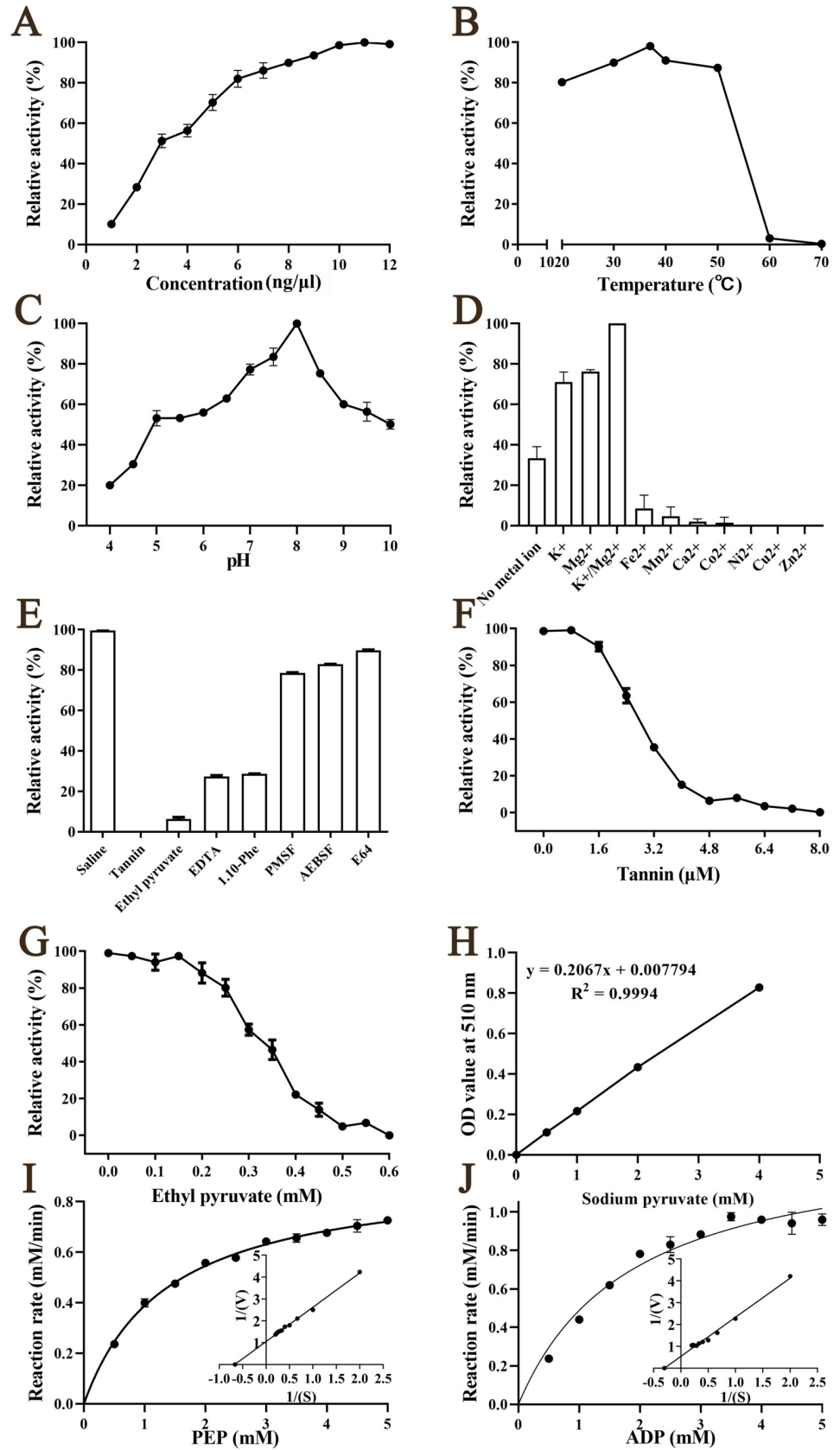


Fig 7. Enzyme activity analysis of rTsPKM. rTsPKM was incubated with 2.5 mM PEP and 1.25 mM ADP for 10 min under various conditions. The optimal catalytic conditions of rTsPKM were assessed with various rTsPKM concentrations (1–12 ng/μl), temperatures (20–70°C) and buffer solution with different pH (4–10). **A:** The optimum catalytic concentration of rTsPKM is 10 ng/μl. **B:** The optimum catalytic temperature of rTsPKM is 37°C. **C:** The optimum catalytic pH of rTsPKM is 8.0. **D:** Effects of different metal ions on rTsPKM activity. K^+ and Mg^{2+} have obvious enhancement role on rTsPKM activity. **E:** Effects of different inhibitors on rTsPKM activity. **F and G:** The suppressive role of tannin (**F**) and ethyl pyruvate (**G**) on rTsPKM activity is dose-dependent. **H:** Standard curve of sodium pyruvate. **I:** Michaelis–Menten curve and Lineweaver–Burk of PEP at pH 8.0 and 37°C. **J:** Michaelis–Menten curve and Lineweaver–Burk of ADP at pH 8.0 and 37°C.

<https://doi.org/10.1371/journal.pntd.0010881.g007>

and the K_m value is 1.51 mM (Fig 7I). The kinetic parameter V_{max} of ADP is 1.84 mM/min and the K_m value is 3.33 mM (Fig 7J).

Suppression of inhibitors on native TsPKM activity in worm somatic proteins

After the ML were treated with various doses of tannin (25, 50, 75 and 100 μM), enzymatic activity of native TsPKM in ML proteins was reduced by 12.82, 20.45, 51.77 and 65.65% respectively, compared to the saline group without incubation using inhibitors ($F = 279.731$, $P < 0.0001$) (Fig 8A). When ethyl pyruvate (10, 20, 30 and 40 mM) was used, native TsPKM enzymatic activity in ML proteins was reduced by 4.76, 14.64, 23.52 and 37.68%, respectively ($F = 205.586$, $P < 0.0001$) (Fig 8B). The native TsPKM activity in ML protein was notable negative correlation with the doses of tannin ($r = -0.978$, $P < 0.01$) and ethyl pyruvate ($r = -0.986$, $P < 0.01$). When the low doses of inhibitors were used, tannin had better inhibitory effect on native TsPKM activity than ethyl pyruvate. Therefore, tannin was used in the subsequent experiments.

Reduction of TsPKM expression and activity after silencing TsPKM gene

After being transfected with 60 ng/μl three dsRNA-TsPKM1, 2, 3 and cultured for 3 days, larval survival of dsRNA-TsPKM1, 2, 3, dsRNA-GFP and PBS group were 93.44, 91.19, 92.63, 92.31 and 93.40%, respectively ($\chi^2 = 0.969$, $P > 0.05$), demonstrating that electroporation had no obvious effect on larval survival. Moreover, dsRNA-TsPKM2 had the strongest suppressive effect on TsPKM transcription and expression among the three kinds of dsRNA ($F = 12.190$,

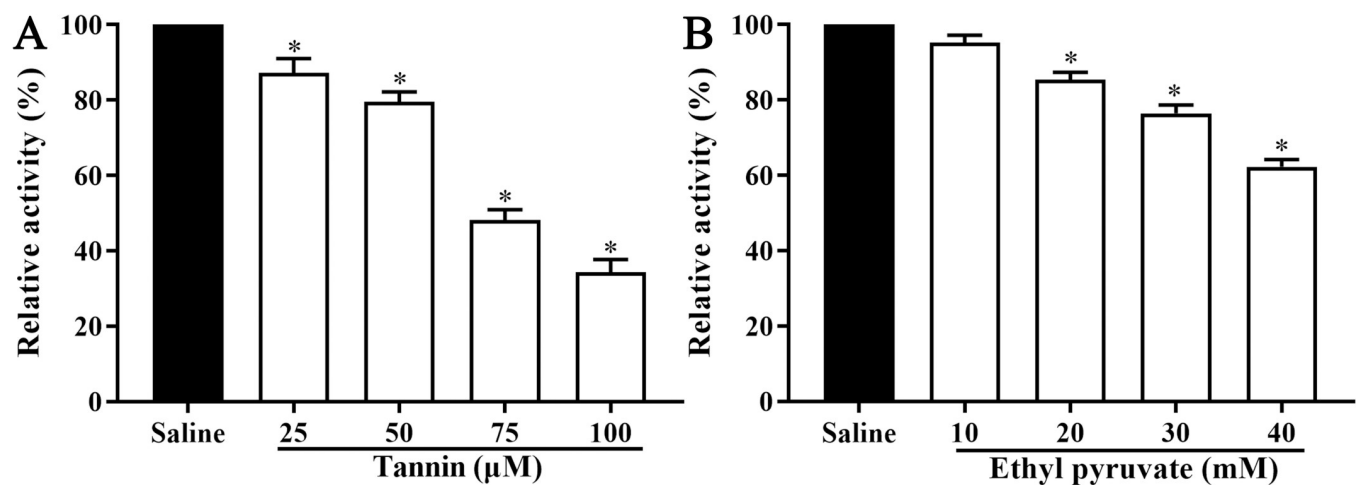


Fig 8. Suppression of tannin (A) and ethyl pyruvate (B) on native TsPKM enzymatic activity in *T. spiralis* muscle larval somatic proteins. * $P < 0.0001$ relative to the saline control group.

<https://doi.org/10.1371/journal.pntd.0010881.g008>

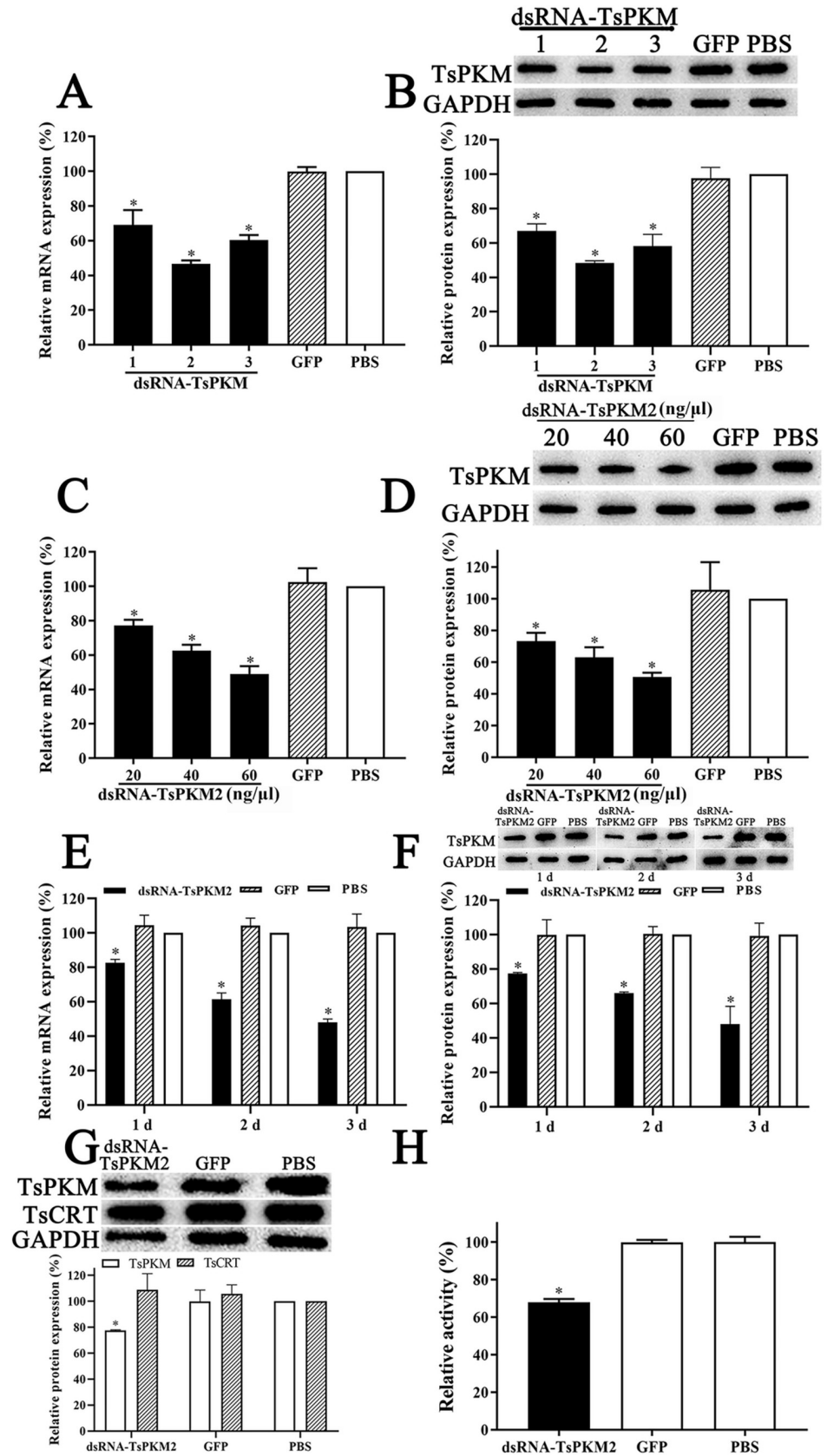


Fig 9. Silencing TsPKM gene suppressed TsPKM expression and enzymatic activity. A: TsPKM transcription levels in ML transfected with different dsRNA-TsPKM. B: TsPKM expression levels in ML transfected with different dsRNA-TsPKM. C: TsPKM transcription levels in ML transfected with various doses of dsRNA-TsPKM2. D: TsPKM expression levels in ML transfected with various doses of dsRNA-TsPKM2. E: TsPKM transcription levels in ML at 1–3 days after transfection with 60 ng/μl dsRNA-TsPKM2. F: TsPKM expression levels in ML at 1–3 days after transfection with 60 ng/μl dsRNA-TsPKM2. G: Expression levels of TsPKM and *Trichinella spiralis* calreticulin (TsCRT) in ML treated using dsRNA-TsPKM2. H: TsPKM enzyme activity in dsRNA-TsPKM2 treated in ML. * $P < 0.05$ relative to the PBS group.

<https://doi.org/10.1371/journal.pntd.0010881.g009>

$P < 0.01$) (Fig 9A and 9B). Therefore, dsRNA-TsPKM2 was used in the following experiment. When the ML were transfected with 20, 40 and 60 ng/μl dsRNA-TsPKM2 and cultured for 3 d, TsPKM mRNA level was reduced by 22.80, 37.30 and 50.91% compared with the PBS group, respectively ($P < 0.05$) (Fig 9C). TsPKM protein expression level was suppressed by 26.81, 36.91 and 49.26% respectively, compared to the PBS group ($P < 0.05$) (Fig 9D). When the ML were transfected with 60 ng/μl dsRNA-TsPKM2 and cultured for 1, 2, 3 d, TsPKM mRNA level was reduced by 17.21, 38.54 and 52.08% compared with the PBS group, respectively ($P < 0.05$) (Fig 9E). TsPKM protein expression level was suppressed by 22.49, 33.85 and 52.03% respectively, compared to the PBS group ($P < 0.05$) (Fig 9F). When the ML were transfected with 60 ng/μl dsRNA-TsPKM2 and cultured for 1 d, *Trichinella spiralis* calreticulin (TsCRT, GenBank: KRY34215.1) protein expression level was not suppressed in ML treated with dsRNA-TsPKM2 (Fig 9G), suggesting that the dsRNA-TsPKM2 is TsPKM-specific. The results of the enzymatic activity assay showed that natural TsPKM enzyme activity in soluble proteins of the ML treated with dsRNA-TsPKM2 was decreased by 26.06% compared to the PBS group ($P < 0.05$) (Fig 9H). Hence, the ML were transfected with 60 ng/μl dsRNA-TsPKM2 and cultured for 3 d in the following experiment.

Suppression of dsRNA-TsPKM on larval glycometabolism

After RNAi treatment, the ATP content of the ML from dsRNA-TsPKM, dsRNA-GFP and PBS groups were 4.1416×10^{-2} , 5.0452×10^{-2} and 5.1958×10^{-2} μM, respectively. Compared to the GFP and PBS group, ATP content in dsRNA-TsPKM treated ML was decreased by 20.29% ($F = 10.916$, $P < 0.05$) (Fig 10A). After tannin treatment, the ATP content was decreased by 43.99% relative to the saline control group ($t = 17.427$, $P < 0.05$) (Fig 10B).

The results of PAS staining showed that glycogen was mainly distributed around the stichosome and intestine of normal ML (Fig 11A and 11B). The total sugar content in ML of

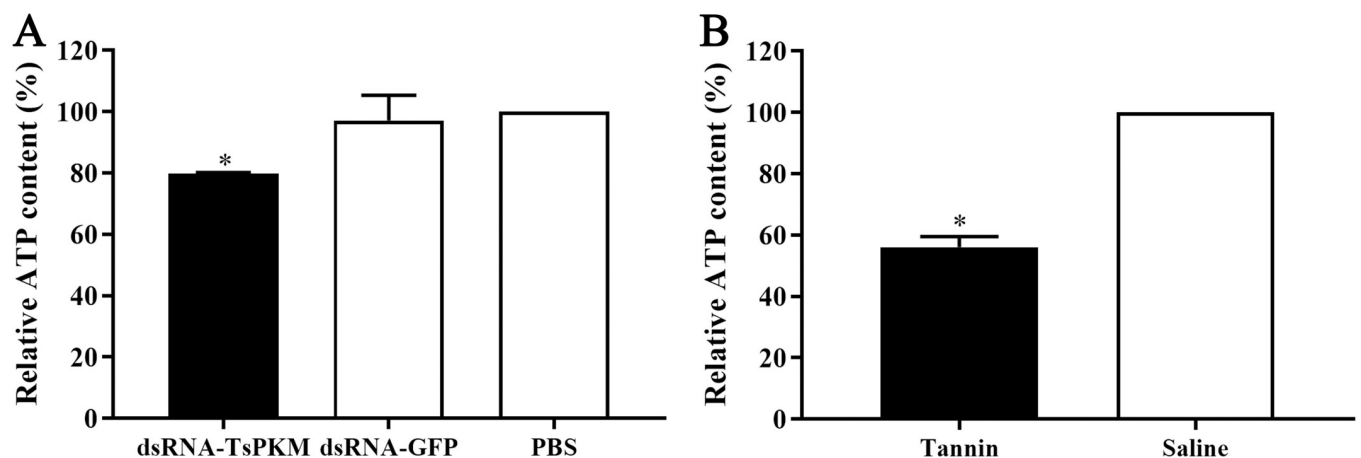


Fig 10. Suppression of dsRNA-TsPKM (A) and tannin (B) on larval ATP content. * $P < 0.05$ relative to the PBS or saline control group.

<https://doi.org/10.1371/journal.pntd.0010881.g010>

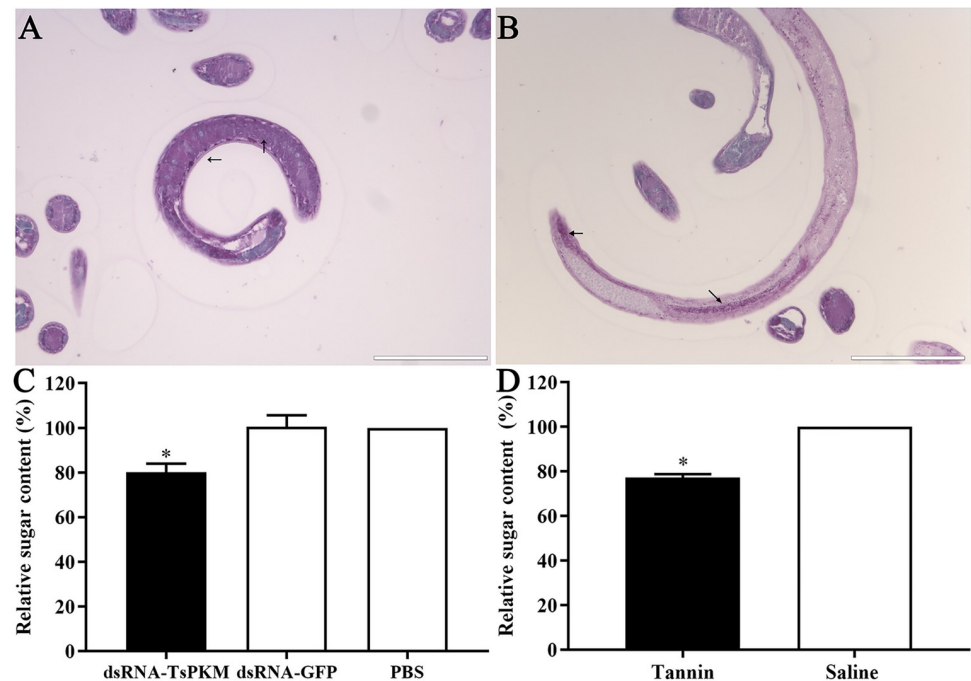


Fig 11. Suppression of dsRNA-TsPKM on *T. spiralis* larval glycometabolism. Glycogen is mainly distributed in the muscle larval stichosome (A) and around the intestine (B). C: dsRNA-TsPKM reduced larval total sugar content. D: Tannin reduced larval total sugar content. The arrows indicate glycogen. * $P < 0.0001$ relative to the PBS or saline group. Scale bars: 100 μm .

<https://doi.org/10.1371/journal.pntd.0010881.g011>

dsRNA-PKM, dsRNA-GFP and PBS groups were 741.8667, 944.5333 and 940.5333 μg respectively. Compared to the GFP and PBS group, total sugar content in ML of dsRNA-PKM group was decreased by 19.86% ($F = 38.611$, $P < 0.0001$). After tannin treatment, the total sugar content in ML was decreased by 22.71% ($t = 29.302$, $P < 0.0001$) (Fig 11C and 11D). The results indicated that TsPKM-specific dsRNA and native inhibitor tannin of pyruvate kinase obviously reduced the sugar content of *T. spiralis* worms, suggesting that pyruvate kinase participates in the glycometabolism of the nematode.

The result of oil red O staining showed that lipid component in intact muscle larvae was dyed red by oil red O, small lipid droplets were thoroughly distributed in the muscle larvae, but there were large lipid droplets in the intestine and tail of the ML (Fig 12A). The darker the red color, the more the lipid content. After treatment with dsRNA and tannin, the larval red color became lighter, suggesting that larval lipid content of treated larvae with dsRNA and tannin was obviously lower than the control groups. The larval lipid content of dsRNA-TsPKM, dsRNA-GFP and PBS groups were 99.825, 150.7 and 152.075 μg respectively. After silencing of larval TsPKM gene by specific dsRNA, larval lipid content in dsRNA-PKM group was decreased by 33.02%, compared to the PBS group ($F = 117.450$, $P < 0.0001$). After tannin treatment, the larval lipid content was decreased by 54.88% ($t = 61.662$, $P < 0.0001$) (Fig 12B and 12C), suggesting that after larval glycometabolism was inhibited by TsPKM-dsRNA, larval lipid metabolism was also impeded.

Inhibition of dsRNA TsPKM on the *in vitro* larval molting

The results of the *in vitro* larval molting assay showed that dsRNA-TsPKM and tannin clearly impeded the larval molting and development of *T. spiralis* (Fig 13A). Larval molting rate of

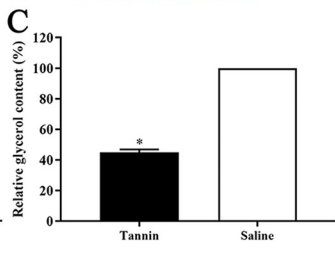
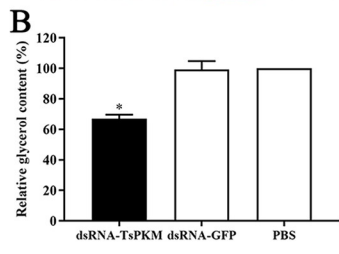
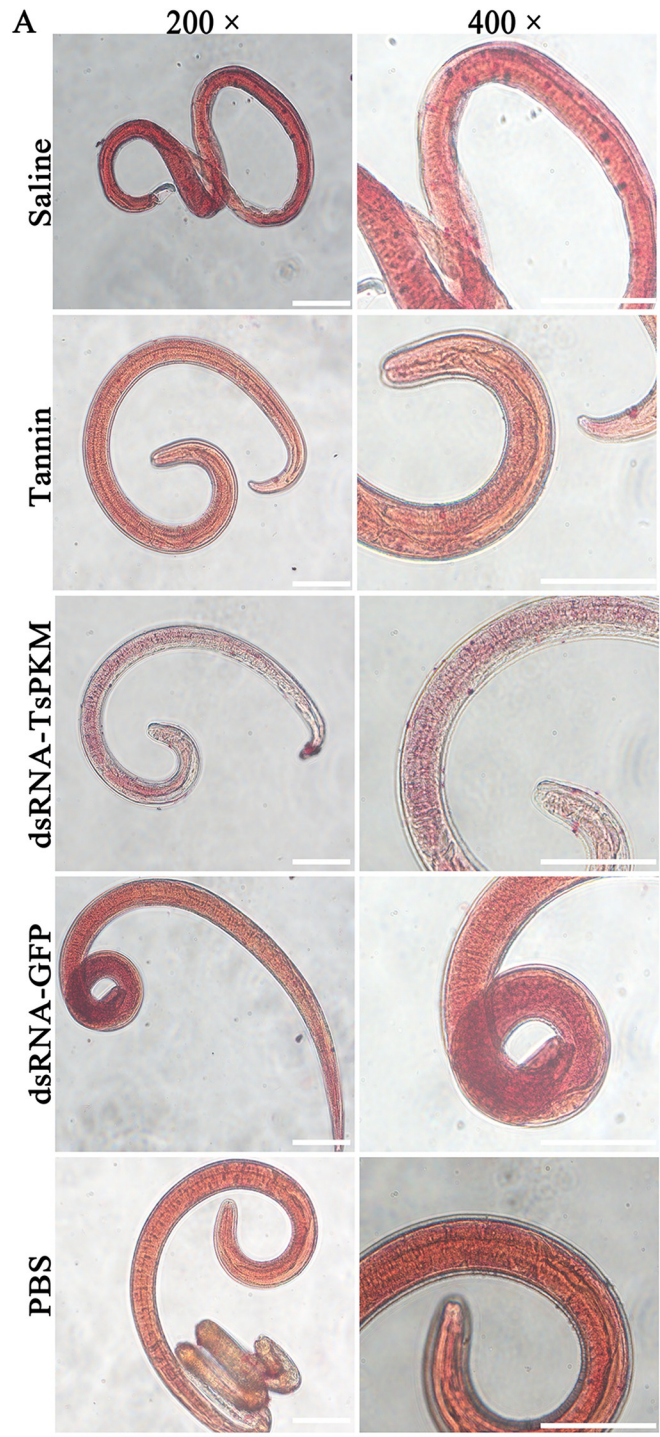


Fig 12. Suppression of dsRNA-TsPKM and tannin on *T. spiralis* larval lipid metabolism **A:** Distribution of lipid droplets in different groups of *T. spiralis* muscle larvae. Small lipid droplets were distributed all over the muscle larvae, but large lipid droplets were principally localized in the larval intestine and tail. After treatment with dsRNA-TsPKM and tannin, the larval red color became lighter, indicating that larval lipid content of treated larvae with dsRNA-TsPKM and tannin was obviously lower than the control groups. **B:** dsRNA-TsPKM decreased larval lipid content, **C:** tannin decreased larval lipid content. * $P < 0.0001$ relative to the PBS or saline group. Scale bars: 100 μm .

<https://doi.org/10.1371/journal.pntd.0010881.g012>

dsRNA-TsPKM, dsRNA-GFP, PBS, tannin and saline groups was 13.33, 20.67, 22.00, 10.67 and 22.67% respectively. Compared with the PBS group, larval molting in the dsRNA-TsPKM group was decreased by 8.67% ($\chi^2 = 3.873$, $P < 0.05$). Compared to the saline group, larval molting of the tannin group was decreased by 12% ($\chi^2 = 7.776$, $P < 0.01$) (Fig 13B). The results suggested that TsPKM also takes part in larval molting and development of the parasite.

Inhibition of RNAi on the *in vivo* larval development and native TsPKM activity

TsPKM-specific dsRNA and tannin obviously restrained the larval growth and development in intestine of infected mice, as demonstrated by shorter and smaller worms recovered from the dsRNA-TsPKM and tannin groups (S1 Fig). Compared to the PBS group, the number of recovered IIL and AW of dsRNA-TsPKM treated group was decreased by 27.69 and 48.57%, respectively ($P < 0.0001$). The number of recovered IIL and AW of tannin-treated group evidently declined too, it was reduced by 43.63 and 44.51%, respectively ($P < 0.0001$) (Fig 14A and 14B). After the ML were treated with RNAi and tannin, the length of the IIL and female and male adults from infected mice was also obviously reduced ($F_{\text{IIL}} = 75.806$, $F_{\text{female}} = 34.329$, $F_{\text{male}} = 37.422$, $P < 0.001$). Compared to the PBS group, the length of IIL, female and male adults of the dsRNA group was decreased by 11.37, 21.40 and 16.75%, respectively ($P < 0.0001$). The length of IIL, female and male adults of the tannin group was reduced by 17.14, 9.30 and 7.09% ($P < 0.0001$) (Fig 14C–14E).

Furthermore, RNAi also remarkably suppressed the enzyme activity of native TsPKM of the IIL and AW recovered from infected mice. Compared to the PBS group, native TsPKM enzyme activity of IIL and AW was decreased by 14.76 and 24.10%, respectively ($P < 0.0001$) (Fig 15). The results suggested that specific silencing TsPKM gene evidently impeded the larval invasion, growth and development, also reduced the native TsPKM activity of the parasite in host's gut.

Suppression of RNAi on the *in vivo* glycometabolism of adult worms

The result of PAS staining showed that glycogen in 3 d AW was mainly distributed in the muscles, stichosome and around intrauterine embryos (S2 Fig). The results of oil red O staining showed that lipid droplets in adult worms were mainly distributed in intrauterine embryos and around intestine (S3 Fig). The sugar content in 3 d AW of dsRNA-TsPKM, dsRNA-GFP, PBS, tannin and saline groups were 624.7111, 620.2667, 533.1556, 622.9333 and 629.1556 μg respectively ($F = 46.371$, $P < 0.0001$). Compared to the PBS group, the sugar content in 3 d AW of dsRNA-TsPKM group was decreased by 14.59% ($P < 0.0001$). But, the sugar content in 3 d AW of the tannin group was basically unchanged compared to the saline group ($P > 0.05$) (Fig 16A). The lipid contents in 3 d AW of dsRNA-TsPKM, dsRNA-GFP, PBS, saline and tannin groups were 553.1167, 540.2833, 426.6167, 536.6167 and 556.7833 μg respectively ($F = 10.802$, $P < 0.01$). The lipid content of dsRNA-TsPKM treated group was decreased by 23.28% relative to the PBS group ($P < 0.0001$), but the lipid content of tannin treated group had no statistical difference compared to the saline control group ($P > 0.05$) (Fig 16B). The results suggested that PKM-specific dsRNA suppressed the glycometabolism in both larval and adult stages.

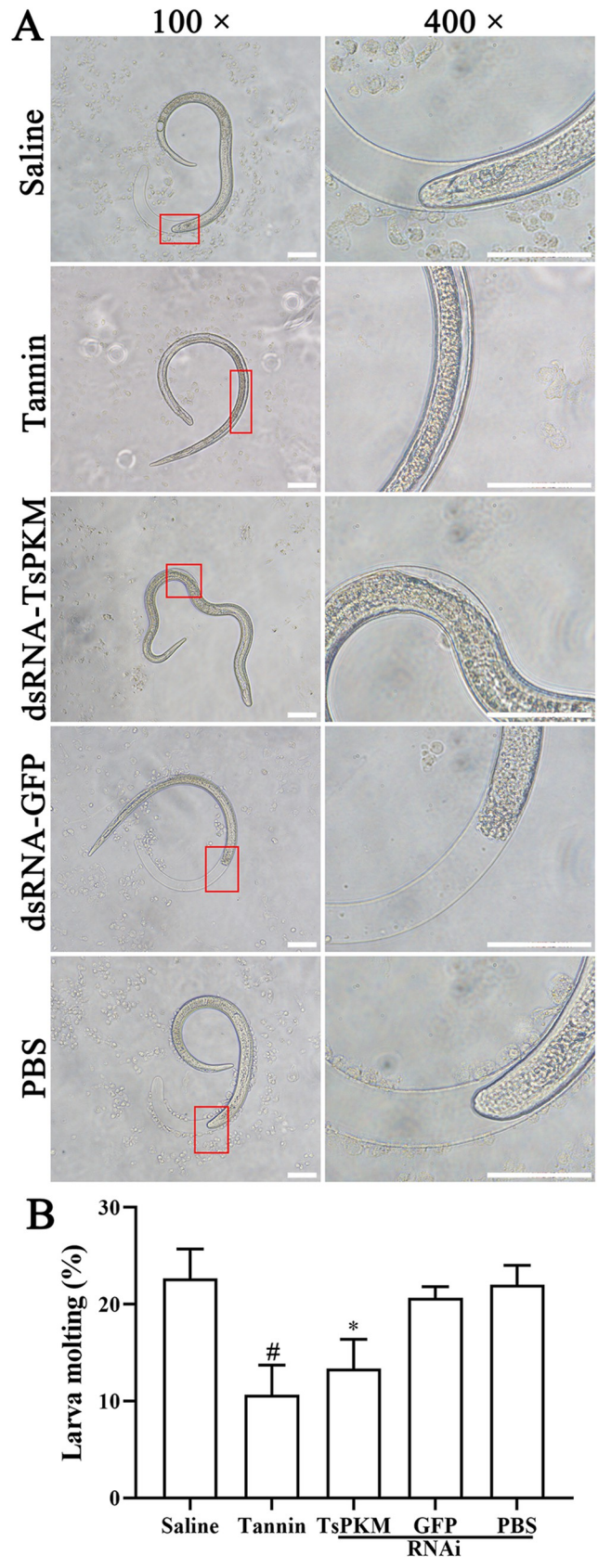


Fig 13. *Trichinella spiralis* larval molting was suppressed by dsRNA-TsPKM in the IIL stage. A: RNAi and tannin significantly inhibited the larval molting, and there was no transparent sheath on both the anterior and tail ends. Especially in the tannin group, there was no obvious separation between old and new cuticles. The area in the red box was enlarged for observation. B: Molting of *T. spiralis* larvae at 3 days after RNAi and tannin treatment. * $P < 0.05$ relative to the PBS group. * $P < 0.01$ relative to the saline group. Scale bars: 200 μm .

<https://doi.org/10.1371/journal.pntd.0010881.g013>

Discussion

At present, albendazole is the first choice for treatment of trichinellosis [73]. Previous studies showed that albendazole has a good killing effect on the intestinal stage of *T. spiralis*, but it has a poor killing effect on NBL and ML stages [74]. Additionally, albendazole has a low bioavailability after oral administration with the recorded values being as low as 5%, and such low bioavailability reduced the chance for successful killing of the migrating and encapsulated larvae [75]. Therefore, it is needed to develop new anti-*Trichinella* drugs. Glycolysis is found to be a good therapeutic target for some parasitic infection, such as *Schistosoma japonicum* [12], *Plasmodium* [15], and so on. Pyruvate kinase as drug target for different parasitic diseases could be verified by gene knockout, RNAi and inhibitors.

In the current study, the complete sequence of TsPKM gene was cloned and expressed in prokaryotic expression system. Sequence analysis revealed that TsPKM had an identity of 98.71, 98.71, 98.53, 98.52, 98.34, 98.34 and 97.79% with pyruvate kinase of the 7 encapsulated *Trichinella* species/genotypes (*T. nativa*, *T. patagoniensis*, *T. murrelli*, *Trichinella* T8, *T. nelsoni*, *T. britovi* and *Trichinella* T6), and it had an identity of 88.89, 88.21 and 88.21% with pyruvate kinase from 3 non-encapsulated *Trichinella* species (*T. pseudospiralis*, *T. papuae* and *T.*

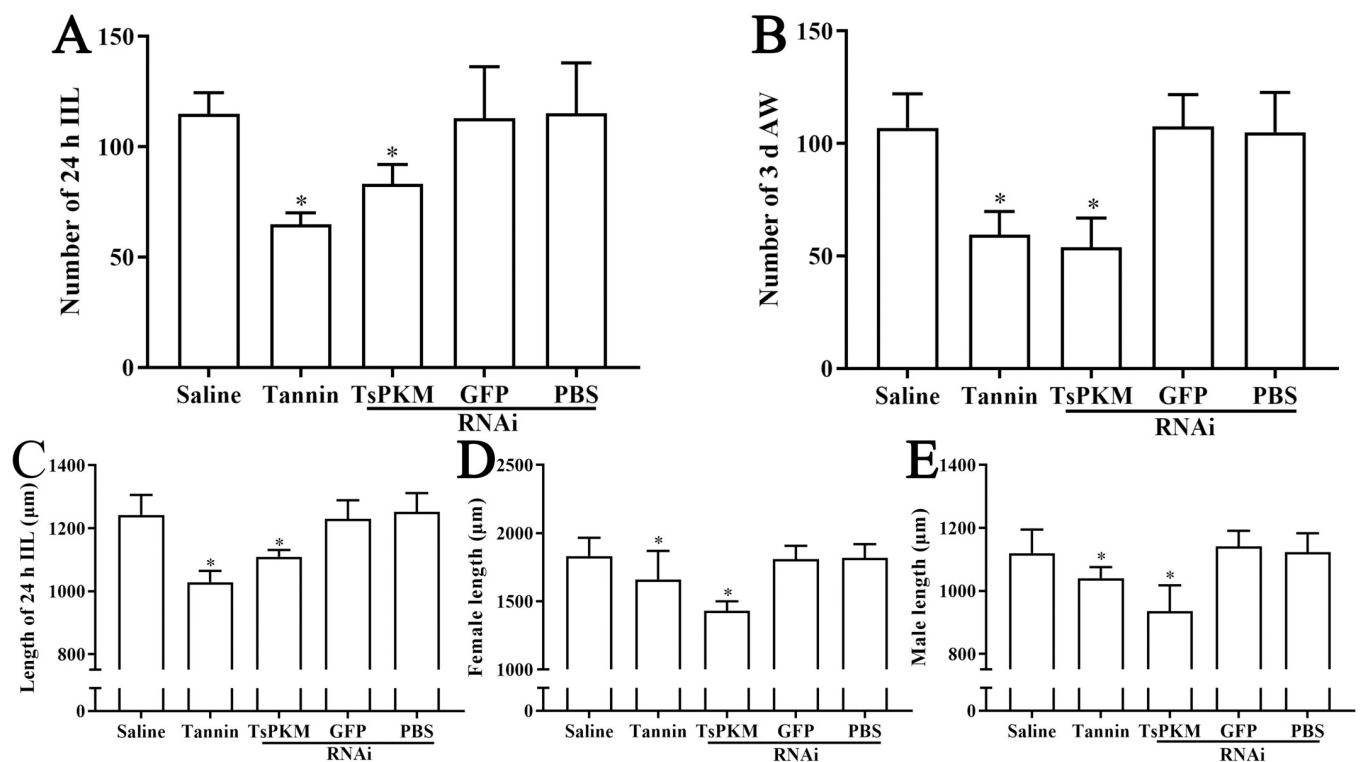


Fig 14. RNAi suppressed the *in vivo* larval development. The numbers of 24 h IIL (A) and 3 d AW (B) collected from intestine of mice infected with the dsRNA-TsPKM and tannin treated ML. The length of 24 h IIL (C) and 3 d female (D) and male adult worms (E) collected from various groups of infected mice. * $P < 0.001$ relative to the PBS or saline control group.

<https://doi.org/10.1371/journal.pntd.0010881.g014>

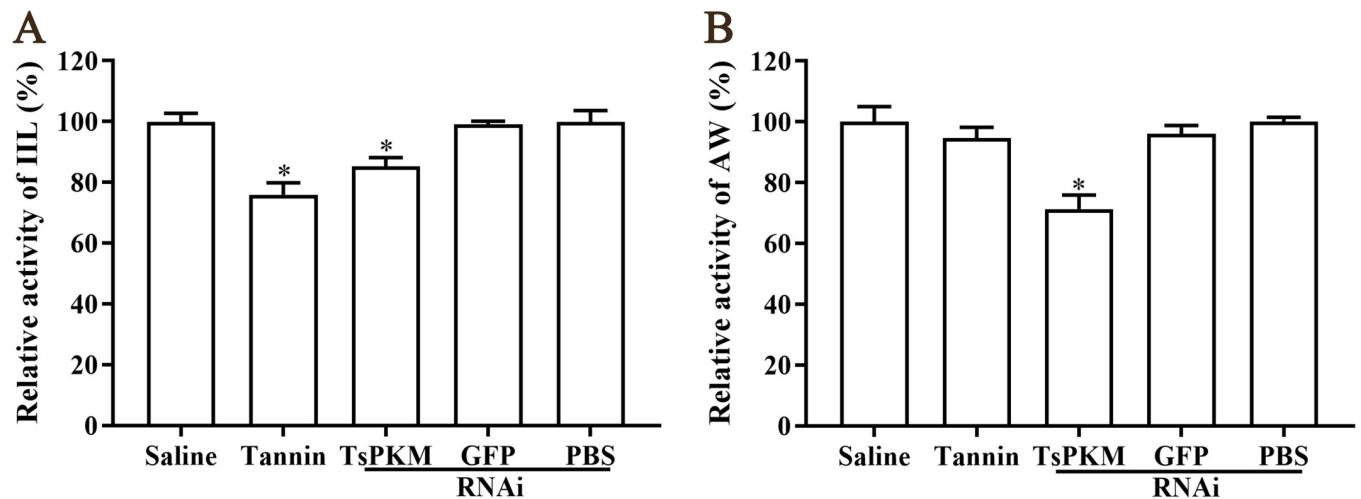


Fig 15. Inhibition of specific dsRNA-TsPKM on native TsPKM enzymatic activity of 24 h IIL (A) and 3 d AW (B) collected from mice challenged with *T. spiralis* ML treated by dsRNA-TsPKM and tannin. * $P < 0.0001$ relative to the PBS or saline control group.

<https://doi.org/10.1371/journal.pntd.0010881.g015>

zimbabwensis). Phylogenetic tree revealed that a monophyletic group of the genus *Trichinella* was well supported. Bioinformatics analysis revealed that the TsPKM belonged to transferases. It had two functional domains of pyruvate kinase, and the enzyme active site. After expression, solubility analysis showed that rTsPKM existed in both supernatant and inclusion body, and the expression level in supernatant was higher. rTsPKM in supernatant was easier to be folded and aggregated correctly, and its protein structure was closer to natural TsPKM, which was more likely to have the catalytic activity function of natural TsPKM [76]. Immunization of mice with rTsPKM induced a specific anti-rTsPKM antibody response, the serum titer of specific anti-rTsPKM IgG reached 1: 10^5 , demonstrating that rTsPKM had a good immunogenicity.

The results of RT-PCR and Western blot showed that TsPKM was transcribed and expressed in various *T. spiralis* stages. The IFT results showed that TsPKM was mainly

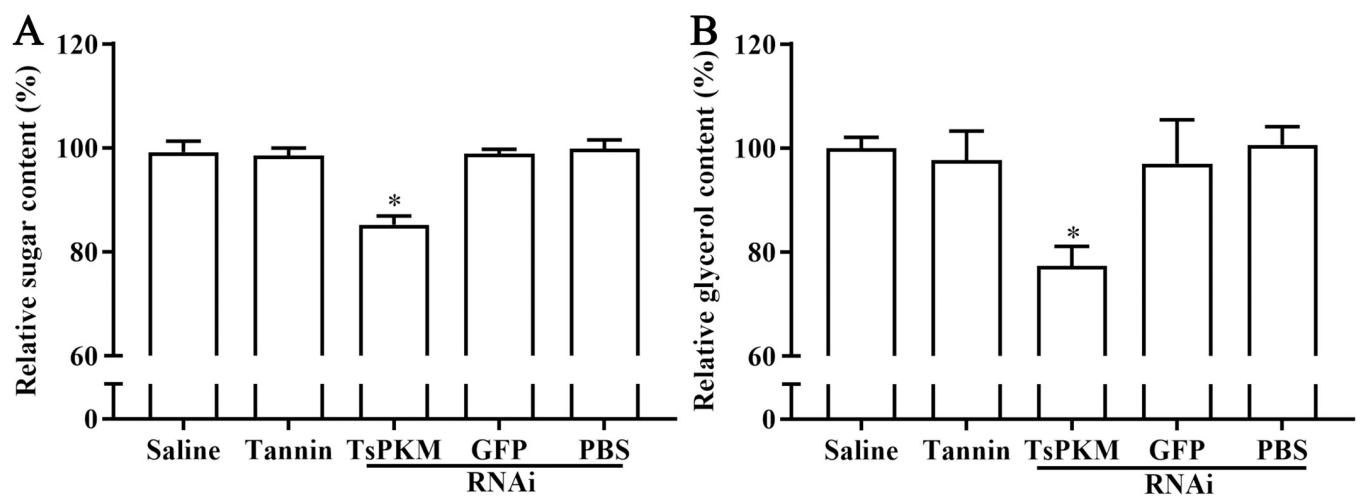


Fig 16. Suppression of dsRNA-TsPKM on sugar and lipid metabolism of *T. spiralis* adult worm from infected mice. dsRNA-TsPKM evidently reduced the content of sugar (A) and lipid (B) in 3 d adult worms. * $P < 0.0001$ relative to the PBS or saline group.

<https://doi.org/10.1371/journal.pntd.0010881.g016>

distributed in the epidermis, muscle cells, stichosome, and intestine and around the embryos. Western blotting results also indicated that rTsPKM was recognized by anti-rTsPKM serum and infected serum, but not by normal mouse serum; natural TsPKM was found in ES proteins of different *T. spiralis* stages. Previous study showed that enzymes of glucose metabolism pathways such as pyruvate kinase exist in ML, 3 d AW and NBL, but the expression level was obviously different in various worm stages, which was related to the different parasitic positions of *T. spiralis* at different stages and the changes of aerobic metabolism and anaerobic metabolism [77]. The pyruvate kinase activity of the ML from freshly killed mice was evidently increased after 60 min-digest and saline incubation for 40 min, suggesting that the activation processes of *T. spiralis* infective ML larvae are stimulated upon liberation of the larvae from the nurse cell inside the host stomach, and the metabolic switch from anaerobic metabolism of infective ML stage to aerobic metabolism was found in the enteral stages [78]. The result of the current study was consistent with the expression of PKM in other parasites, which was mainly distributed in tissues with high energy metabolism, such as muscle and rapid embryo proliferation [13,79]. Our results indicated that TsPKM was expressed in various *T. spiralis* stages and it was a secretory protein, demonstrated that TsPKM is a necessary protein in *T. spiralis* lifecycle and might participate in larval molting, sugar metabolism, development and reproduction of this parasite [72]. The results suggested that secretory TsPKM could be exposed directly to host's immune system and trigger the production of anti-TsPKM antibodies during *T. spiralis* infection [80,81].

The enzyme activity of rTsPKM was detected by 2,4-dinitrophenylhydrazine chromogenic method, the results showed that rTsPKM expressed in this study had the catalytic activity of natural pyruvate kinase. In the buffer system, metal ions K^+ and Mg^{2+} significantly enhanced the enzyme activity of rTsPKM, suggesting that K^+ and Mg^{2+} played an indispensable role in the activity of pyruvate kinase. K^+ and Mg^{2+} hardly affect the structure of pyruvate kinase, however the domain can be reversed under the action of K^+ and Mg^{2+} , which made the active site of pyruvate kinase more exposed [82]. For different concentrations of ethyl pyruvate and tannin, the inhibition roles were increased with the increase of inhibitor concentration. rTsPKM enzyme activity was completely inhibited by 0.60 mM ethyl pyruvate and 8 μ M tannin. In tumor tissues, the proliferation of tumor cells was through K433 site of PKM2, and tannin selectively inhibits the pyruvate kinase activity of PKM2, rather than protein kinase activity and PKM2 expression, to suppress colorectal cancer cell proliferation, tannin is a promising PKM2 inhibitor for prevention of colorectal cancer [83]. Ethyl pyruvate also has a good inhibitory effect on PKM, it is safe for red blood cells and easy to penetrate the blood-brain barrier [56]. In *Trypanosoma brucei*, 5 mM ethyl pyruvate incubated with trypanosomes for 3 h can completely inhibit the proliferation of trypanosomes and kill trypanosomes [56]. Tannin and ethyl pyruvate inhibited the enzymatic activity of pyruvate kinase in *Trichinella spiralis* and other parasites, but the difference of effective inhibitory concentrations may be related with the size and parasitic site of the parasites.

RNAi has been widely used for study on the gene function of various parasites [60]. In order to further verify the function of TsPKM in the sugar metabolism, growth and development of this nematode, RNAi and tannin were used in this study. After treatment with 60 ng/ μ l of dsRNA-PKM2 for 3 days and 100 μ M tannin for 2 hours, the catalytic activity of TsPKM, ATP content, total sugar content and lipid content in ML distinctly decreased, suggesting that RNAi and tannin suppressed larval sugar metabolism, reduced ATP production. Molting is the most significant feature of intestinal larval development in *T. spiralis* lifecycle [84]. In the present study, the *in vitro* IIL molting was evidently inhibited by RNAi and tannin treatment. The results of animal challenge experiments showed that the number and length of 24 h IIL and 3 d AW and the content of total sugar and lipid in 3 d AW in dsRNA TsPKM group were

significantly reduced and inhibited. Furthermore, RNAi also remarkably suppressed the enzyme activity of native TsPKM of the IIL and AW recovered from infected mice. The results further confirmed that TsPKM played an important role in the larval molting, metabolism, growth and development of this parasite. In previous studies on other parasites, inhibition of pyruvate kinase led to the decline of ATP level, metabolic disorder and obvious inhibition of larval growth and development of larvae. The inhibition of pyruvate kinase expression in *Giardia canis* using specific hammerhead ribozyme decreased pyruvate kinase enzyme activity and impaired growth and development of *G. canis* trophozoites [85]. Knockout of PYK1 and PYK2 genes by CRISPR/Cas9 technology completely hindered the growth and caused the death of *Toxoplasma gondii* [16]. The results suggested that pyruvate kinase might be a potential candidate drug target against *Trichinella* infection.

In conclusion, a novel TsPKM was cloned and expressed, its biological characteristics and roles in sugar metabolism, larval molting and development of *T. spiralis* were investigated in this study. The results showed that TsPKM was transcribed and expressed at various *T. spiralis* developmental stages, mainly localized at cuticle, muscle layer, stichosome, intestine and around the embryos. The rTsPKM had the native enzymatic activity of pyruvate kinase to catalyze the reaction of PEP and ADP. The silencing of TsPKM gene by TsPKM-specific dsRNA significantly reduced the expression levels and enzyme activity of native TsPKM in the larvae, and RNAi also suppressed larval molting, sugar metabolism, growth and development of this parasite. The results indicated that TsPKM is an obligatory enzyme in *T. spiralis* lifecycle; it was involved in larval molting, sugar metabolism and development, and may be regarded as a potential candidate drug target against *T. spiralis* infection.

Supporting information

S1 Fig. Morphology of the IIL and adult worms recovered from mice challenged with *T. spiralis* ML treated with dsRNA-TsPKM and tannin. Scale bars: 200 μm . (JPG)

S2 Fig. Distribution of glycogen in cross-sections of 3 d adult worms from different groups of infected mice. A: Saline group. B: Tannin group. C and D: dsRNA-TsPKM group. E: dsRNA-GFP group. F: PBS group. Glycogen of 3 d AW is mainly distributed in muscles, stichosome and around intrauterine embryos. Black arrows indicate the glycogen. Scale bars: 100 μm . (JPG)

S3 Fig. Distribution of lipid droplets in whole adult worms of different groups of infected mice at 3 days post infection. Lipid droplets were mainly distributed in intrauterine embryos and around intestine of adult worms. Scale bars: 200 μm . (JPG)

Author Contributions

Conceptualization: Zhong Quan Wang, Jing Cui.

Data curation: Wen Wen Yue.

Funding acquisition: Jing Cui.

Investigation: Wen Wen Yue, Shu Wei Yan, Ru Zhang, Yong Kang Cheng, Ruo Dan Liu, Shao Rong Long, Xi Zhang, Zhong Quan Wang, Jing Cui.

Methodology: Wen Wen Yue, Zhong Quan Wang, Jing Cui.

Project administration: Zhong Quan Wang, Jing Cui.

Resources: Zhong Quan Wang, Jing Cui.

Supervision: Zhong Quan Wang, Jing Cui.

Writing – original draft: Wen Wen Yue, Zhong Quan Wang, Jing Cui.

Writing – review & editing: Wen Wen Yue, Zhong Quan Wang, Jing Cui.

References

1. van der Giessen J, Deksne G, Gomez-Morales MA, Troell K, Gomes J, Sotiraki S, et al. Surveillance of foodborne parasitic diseases in Europe in a One Health approach. *Parasite Epidemiol Control*. 2021; 13: e00205. <https://doi.org/10.1016/j.parepi.2021.e00205> PMID: 33665388
2. Zhang XZ, Wang ZQ, Cui J. Epidemiology of trichinellosis in the People's Republic of China during 2009–2020. *Acta Trop*. 2022; 229: 106388. <https://doi.org/10.1016/j.actatropica.2022.106388> PMID: 35231417
3. Cui J, Jiang P, Liu LN, Wang ZQ. Survey of *Trichinella* infections in domestic pigs from northern and eastern Henan, China. *Vet Parasitol*. 2013; 194(2–4): 133–5. <https://doi.org/10.1016/j.vetpar.2013.01.038> PMID: 23422779
4. Jiang P, Zhang X, Wang LA, Han LH, Yang M, Duan JY, et al. Survey of *Trichinella* infection from domestic pigs in the historical endemic areas of Henan province, central China. *Parasitol Res*. 2016; 115(12): 4707–9. <https://doi.org/10.1007/s00436-016-5240-x> PMID: 27601238
5. Rostami A, Gamble HR, Dupouy-Camet J, Khazan H, Bruschi F. Meat sources of infection for outbreaks of human trichinellosis. *Food Microbiol*. 2017; 64: 65–71. <https://doi.org/10.1016/j.fm.2016.12.012> PMID: 28213036
6. Ren HJ, Cui J, Yang W, Liu RD, Wang ZQ. Identification of differentially expressed genes of *Trichinella spiralis* larvae after exposure to host intestine milieu. *PLoS One*. 2013; 8(6): e67570. <https://doi.org/10.1371/journal.pone.0067570> PMID: 23840742
7. Liu RD, Jiang P, Wen H, Duan JY, Wang LA, Li JF, et al. Screening and characterization of early diagnostic antigens in excretory-secretory proteins from *Trichinella spiralis* intestinal infective larvae by immunoproteomics. *Parasitol Res*. 2016; 115(2): 615–22. <https://doi.org/10.1007/s00436-015-4779-2> PMID: 26468148
8. Despommier DD. How does *Trichinella spiralis* make itself at home? *Parasitol Today*. 1998; 14(8): 318–23. [https://doi.org/10.1016/s0169-4758\(98\)01287-3](https://doi.org/10.1016/s0169-4758(98)01287-3) PMID: 17040798
9. Ferguson JD, Castro GA. Metabolism of intestinal stages of *Trichinella spiralis*. *Am J Physiol*. 1973; 225(1): 85–9. <https://doi.org/10.1152/ajplegacy.1973.225.1.85> PMID: 4736619
10. Gray LR, Sultana MR, Rauckhorst AJ, Oonthonpan L, Tompkins SC, Sharma A, et al. Hepatic mitochondrial pyruvate carrier 1 is required for efficient regulation of gluconeogenesis and whole-body glucose homeostasis. *Cell Metab*. 2015; 22(4): 669–81. <https://doi.org/10.1016/j.cmet.2015.07.027> PMID: 26344103
11. Watts JL, Ristow M. Lipid and carbohydrate metabolism in *Caenorhabditis elegans*. *Genetics*. 2017; 207(2): 413–46. <https://doi.org/10.1534/genetics.117.300106> PMID: 28978773
12. Xiao SH, You JQ, Guo HF, Jiao PY, Mei JY, Yao MY, et al. Effect of artemether on glyceraldehyde-3-phosphate dehydrogenase, phosphoglycerate kinase, and pyruvate kinase of *Schistosoma japonicum* harbored in mice. *Zhongguo Yao Li Xue Bao*. 1998; 19(3): 279–81. PMID: 10375745
13. Das B, Ramnath, Dutta AK, Tandon V. Differential kinetics at PK/PEPCK branch point in the cestode, *Raillietina echinobothrida*. *Exp Parasitol*. 2015; 153: 151–9. <https://doi.org/10.1016/j.exppara.2015.03.023> PMID: 25816970
14. Dan M, Wang CC. Role of alcohol dehydrogenase E (ADHE) in the energy metabolism of *Giardia lamblia*. *Mol Biochem Parasitol*. 2000; 109(1): 25–36. [https://doi.org/10.1016/s0166-6851\(00\)00233-4](https://doi.org/10.1016/s0166-6851(00)00233-4) PMID: 10924754
15. Zhong W, Li K, Cai Q, Guo J, Yuan M, Wong YH, et al. Pyruvate kinase from *Plasmodium falciparum*: Structural and kinetic insights into the allosteric mechanism. *Biochem Biophys Res Commun*. 2020; 532(3): 370–6. <https://doi.org/10.1016/j.bbrc.2020.08.048> PMID: 32878705
16. Xia N, Ye S, Liang X, Chen P, Zhou Y, Fang R, et al. Pyruvate homeostasis as a determinant of parasite growth and metabolic plasticity in *Toxoplasma gondii*. *mBio*. 2019; 10(3). <https://doi.org/10.1128/mBio.00898-19> PMID: 31186321

17. Khan SM, Zhang X, Witola WH. *Cryptosporidium parvum* pyruvate kinase inhibitors with in vivo anti-cryptosporidial efficacy. *Front Microbiol.* 2021; 12: 800293. <https://doi.org/10.3389/fmicb.2021.800293> PMID: 35046922
18. Mitreva M, Jasmer DP, Zarlenga DS, Wang Z, Abubucker S, Martin J, et al. The draft genome of the parasitic nematode *Trichinella spiralis*. *Nat Genet.* 2011; 43(3): 228–35. <https://doi.org/10.1038/ng.769> PMID: 21336279
19. Clower CV, Chatterjee D, Wang Z, Cantley LC, Vander Heiden MG, Krainer AR. The alternative splicing repressors hnRNP A1/A2 and PTB influence pyruvate kinase isoform expression and cell metabolism. *Proc Natl Acad Sci U S A.* 2010; 107(5): 1894–9. <https://doi.org/10.1073/pnas.0914845107> PMID: 20133837
20. Wang ZQ, Li LZ, Jiang P, Liu LN, Cui J. Molecular identification and phylogenetic analysis of *Trichinella* isolates from different provinces in mainland China. *Parasitol Res.* 2012; 110(2): 753–7. <https://doi.org/10.1007/s00436-011-2549-3> PMID: 21773771
21. Ren HJ, Liu RD, Wang ZQ, Cui J. Construction and use of a *Trichinella spiralis* phage display library to identify the interactions between parasite and host enterocytes. *Parasitol Res.* 2013; 112(5): 1857–63. <https://doi.org/10.1007/s00436-013-3339-x> PMID: 23420409.
22. Li JF, Guo KX, Qi X, Lei JJ, Han Y, Yan SW, et al. Protective immunity against *Trichinella spiralis* in mice elicited by oral vaccination with attenuated *Salmonella*-delivered TsSP1.2 DNA. *Vet Res.* 2018; 49(1): 87. <https://doi.org/10.1186/s13567-018-0582-2> PMID: 30189894
23. Jiang P, Wang ZQ, Cui J, Zhang X. Comparison of artificial digestion and Baermann's methods for detection of *Trichinella spiralis* pre-encapsulated larvae in muscles with low-level infections. *Foodborne Pathog Dis.* 2012; 9(1): 27–31. <https://doi.org/10.1089/fpd.2011.0985> PMID: 21988397
24. Liu RD, Cui J, Liu XL, Jiang P, Sun GG, Zhang X, et al. Comparative proteomic analysis of surface proteins of *Trichinella spiralis* muscle larvae and intestinal infective larvae. *Acta Trop.* 2015; 150: 79–86. <https://doi.org/10.1016/j.actatropica.2015.07.002> PMID: 26184560
25. Sun GG, Liu RD, Wang ZQ, Jiang P, Wang L, Liu XL, et al. New diagnostic antigens for early trichinellosis: the excretory-secretory antigens of *Trichinella spiralis* intestinal infective larvae. *Parasitol Res.* 2015; 114(12): 4637–44. <https://doi.org/10.1007/s00436-015-4709-3> PMID: 26342828
26. Sun GG, Wang ZQ, Liu CY, Jiang P, Liu RD, Wen H, et al. Early serodiagnosis of trichinellosis by ELISA using excretory-secretory antigens of *Trichinella spiralis* adult worms. *Parasit Vectors.* 2015; 8: 484. <https://doi.org/10.1186/s13071-015-1094-9> PMID: 26394626
27. Hu YY, Zhang R, Yan SW, Yue WW, Zhang JH, Liu RD, et al. Characterization of a novel cysteine protease in *Trichinella spiralis* and its role in larval intrusion, development and fecundity. *Vet Res.* 2021; 52(1): 113. <https://doi.org/10.1186/s13567-021-00983-1> PMID: 34446106
28. Guo KX, Bai Y, Ren HN, Sun XY, Song YY, Liu RD, et al. Characterization of a *Trichinella spiralis* aminopeptidase and its participation in invasion, development and fecundity. *Vet Res.* 2020; 51(1): 78. <https://doi.org/10.1186/s13567-020-00805-w> PMID: 32539772
29. Wu Z, Nagano I, Takahashi Y, Maekawa Y. Practical methods for collecting *Trichinella* parasites and their excretory-secretory products. *Parasitol Int.* 2016; 65(5 Pt B): 591–5. <https://doi.org/10.1016/j.parint.2016.08.001> PMID: 27495839
30. Korhonen PK, Pozio E, La Rosa G, Chang BC, Koehler AV, Hoberg EP, et al. Phylogenomic and biogeographic reconstruction of the *Trichinella* complex. *Nat Commun.* 2016; 7: 10513. <https://doi.org/10.1038/ncomms10513> PMID: 26830005
31. Li LG, Wang ZQ, Liu RD, Yang X, Liu LN, Sun GG, et al. *Trichinella spiralis*: low vaccine potential of glutathione S-transferase against infections in mice. *Acta Trop.* 2015; 146: 25–32. <https://doi.org/10.1016/j.actatropica.2015.02.020> PMID: 25757368
32. Bai Y, Ma KN, Sun XY, Dan Liu R, Long SR, Jiang P, et al. Molecular characterization of a novel cathepsin L from *Trichinella spiralis* and its participation in invasion, development and reproduction. *Acta Trop.* 2021; 224: 106112. <https://doi.org/10.1016/j.actatropica.2021.106112> PMID: 34453915
33. Lei JJ, Hu YY, Liu F, Yan SW, Liu RD, Long SR, et al. Molecular cloning and characterization of a novel peptidase from *Trichinella spiralis* and protective immunity elicited by the peptidase in BALB/c mice. *Vet Res.* 2020; 51(1): 111. <https://doi.org/10.1186/s13567-020-00838-1> PMID: 32891183
34. Sun XY, Ma KN, Bai Y, Liu RD, Long SR, Zhang X, et al. Molecular cloning and characterization of a novel aspartyl aminopeptidase from *Trichinella spiralis*. *Trop Biomed.* 2021; 38(3): 420–34. <https://doi.org/10.47665/tb.38.3.085> PMID: 34608116
35. Ren HN, Bai SJ, Wang Z, Han LL, Yan SW, Jiang P, et al. A metalloproteinase Tsdpy31 from *Trichinella spiralis* participates in larval molting and development. *Int J Biol Macromol.* 2021; 192: 883–94. <https://doi.org/10.1016/j.ijbiomac.2021.10.021> PMID: 34656542

36. Xu J, Yang F, Yang DQ, Jiang P, Liu RD, Zhang X, et al. Molecular characterization of *Trichinella spiralis* galectin and its participation in larval invasion of host's intestinal epithelial cells. *Vet Res.* 2018; 49(1): 79. <https://doi.org/10.1186/s13567-018-0573-3> PMID: 30068382
37. Sun GG, Song YY, Jiang P, Ren HN, Yan SW, Han Y, et al. Characterization of a *Trichinella spiralis* putative serine protease. Study of its potential as sero-diagnostic tool. *PLoS Negl Trop Dis.* 2018; 12(5): e0006485. <https://doi.org/10.1371/journal.pntd.0006485> PMID: 29758030
38. Xu J, Liu RD, Bai SJ, Hao HN, Yue WW, Xu YXY, et al. Molecular characterization of a *Trichinella spiralis* aspartic protease and its facilitation role in larval invasion of host intestinal epithelial cells. *PLoS Negl Trop Dis.* 2020; 14(4): e0008269. <https://doi.org/10.1371/journal.pntd.0008269> PMID: 32339171
39. Zhang XZ, Sun XY, Bai Y, Song YY, Hu CX, Li X, et al. Protective immunity in mice vaccinated with a novel elastase-1 significantly decreases *Trichinella spiralis* fecundity and infection. *Vet Res.* 2020; 51(1): 43. <https://doi.org/10.1186/s13567-020-00767-z> PMID: 32169101
40. Cui J, Ren HJ, Liu RD, Wang L, Zhang ZF, Wang ZQ. Phage-displayed specific polypeptide antigens induce significant protective immunity against *Trichinella spiralis* infection in BALB/c mice. *Vaccine.* 2013; 31(8): 1171–7. <https://doi.org/10.1016/j.vaccine.2012.12.070> PMID: 23306358
41. Cui J, Wang L, Sun GG, Liu LN, Zhang SB, Liu RD, et al. Characterization of a *Trichinella spiralis* 31 kDa protein and its potential application for the serodiagnosis of trichinellosis. *Acta Trop.* 2015; 142: 57–63. <https://doi.org/10.1016/j.actatropica.2014.10.017> PMID: 25447831
42. Ren HN, Guo KX, Zhang Y, Sun GG, Liu RD, Jiang P, et al. Molecular characterization of a 31 kDa protein from *Trichinella spiralis* and its induced immune protection in BALB/c mice. *Parasit Vectors.* 2018; 11(1): 625. <https://doi.org/10.1186/s13071-018-3198-5> PMID: 30518426
43. Liu CY, Song YY, Ren HN, Sun GG, Liu RD, Jiang P, et al. Cloning and expression of a *Trichinella spiralis* putative glutathione S-transferase and its elicited protective immunity against challenge infections. *Parasit Vectors.* 2017; 10(1): 448. <https://doi.org/10.1186/s13071-017-2384-1> PMID: 28962639
44. Qi X, Yue X, Han Y, Jiang P, Yang F, Lei JJ, et al. Characterization of two *Trichinella spiralis* adult-specific DNase II and their capacity to induce protective immunity. *Front Microbiol.* 2018; 9: 2504. <https://doi.org/10.3389/fmicb.2018.02504> PMID: 30455671
45. Zhuo TX, Wang Z, Song YY, Yan SW, Liu RD, Zhang X, et al. Characterization of a novel glutamine synthetase from *Trichinella spiralis* and its participation in larval acid resistance, molting, and development. *Front Cell Dev Biol.* 2021; 9: 729402. <https://doi.org/10.3389/fcell.2021.729402> PMID: 34616735
46. Wang B, Wang ZQ, Jin J, Ren HJ, Liu LN, Cui J. Cloning, expression and characterization of a *Trichinella spiralis* serine protease gene encoding a 35.5 kDa protein. *Exp Parasitol.* 2013; 134(2): 148–54. <https://doi.org/10.1016/j.exppara.2013.03.004> PMID: 23501807
47. Zhang Y, Wang Z, Li L, Cui J. Molecular characterization of *Trichinella spiralis* aminopeptidase and its potential as a novel vaccine candidate antigen against trichinellosis in BALB/c mice. *Parasit Vectors.* 2013; 6: 246. <https://doi.org/10.1186/1756-3305-6-246> PMID: 23972034
48. Xu J, Liu RD, Long SR, Song YY, Jiang P, Zhang X, et al. Characterization of a chymotrypsin-like enzyme from *Trichinella spiralis* and its facilitation of larva penetration into the host's enteral epithelial cells. *Res Vet Sci.* 2020; 128: 1–8. <https://doi.org/10.1016/j.rvsc.2019.10.018> PMID: 31706217
49. Long SR, Wang ZQ, Jiang P, Liu RD, Qi X, Liu P, et al. Characterization and functional analysis of *Trichinella spiralis* Nudix hydrolase. *Exp Parasitol.* 2015; 159: 264–73. <https://doi.org/10.1016/j.exppara.2015.10.009> PMID: 26545353
50. Yue X, Sun XY, Liu F, Hu CX, Bai Y, Da Yang Q, et al. Molecular characterization of a *Trichinella spiralis* serine proteinase. *Vet Res.* 2020; 51(1): 125. <https://doi.org/10.1186/s13567-020-00847-0> PMID: 32988413
51. Cui J, Han Y, Yue X, Liu F, Song YY, Yan SW, et al. Vaccination of mice with a recombinant novel cathepsin B inhibits *Trichinella spiralis* development, reduces the fecundity and worm burden. *Parasit Vectors.* 2019; 12(1): 581. <https://doi.org/10.1186/s13071-019-3833-9> PMID: 31829230
52. Qi X, Han Y, Jiang P, Yue X, Ren HN, Sun GG, et al. Oral vaccination with *Trichinella spiralis* DNase II DNA vaccine delivered by attenuated *Salmonella* induces a protective immunity in BALB/c mice. *Vet Res.* 2018; 49(1): 119. <https://doi.org/10.1186/s13567-018-0614-y> PMID: 30518422
53. Hu CX, Xu YXY, Hao HN, Liu RD, Jiang P, Long SR, et al. Oral vaccination with recombinant *Lactobacillus plantarum* encoding *Trichinella spiralis* inorganic pyrophosphatase elicited a protective immunity in BALB/c mice. *PLoS Negl Trop Dis.* 2021; 15(10): e0009865. <https://doi.org/10.1371/journal.pntd.0009865> PMID: 34699522
54. Cui J, Li LG, Jiang P, Liu RD, Yang X, Liu LN, et al. Biochemical and functional characterization of the glutathione S-transferase from *Trichinella spiralis*. *Parasitol Res.* 2015; 114(5): 2007–13. <https://doi.org/10.1007/s00436-015-4410-6> PMID: 25758588

55. Hu CX, Zeng J, Hao HN, Xu YXY, Liu F, Liu RD, et al. Biological properties and roles of a *Trichinella spiralis* inorganic pyrophosphatase in molting and developmental process of intestinal larval stages. *Vet Res.* 2021; 52(1): 6. <https://doi.org/10.1186/s13567-020-00877-8> PMID: 33413587
56. Worku N, Stich A, Dauschies A, Wenzel I, Kurz R, Thieme R, et al. Ethyl pyruvate emerges as a safe and fast acting agent against *Trypanosoma brucei* by targeting pyruvate kinase activity. *PLoS One.* 2015; 10(9): e0137353. <https://doi.org/10.1371/journal.pone.0137353> PMID: 26340747
57. Song YY, Lu QQ, Han LL, Yan SW, Zhang XZ, Liu RD, et al. Proteases secreted by *Trichinella spiralis* intestinal infective larvae damage the junctions of the intestinal epithelial cell monolayer and mediate larval invasion. *Vet Res.* 2022; 53(1): 19. <https://doi.org/10.1186/s13567-022-01032-1> PMID: 35255974
58. Zhong RZ, Sun HX, Liu HW, Zhou DW. Effects of tannic acid on *Haemonchus contortus* larvae viability and immune responses of sheep white blood cells in vitro. *Parasite Immunol.* 2014; 36(2): 100–6. <https://doi.org/10.1111/pim.12092> PMID: 24558656
59. Yang W, Li LG, Liu RD, Sun GG, Liu CY, Zhang SB, et al. Molecular identification and characterization of *Trichinella spiralis* proteasome subunit beta type-7. *Parasit Vectors.* 2015; 8: 18. <https://doi.org/10.1186/s13071-014-0626-z> PMID: 25582125
60. Zhang SB, Jiang P, Wang ZQ, Long SR, Liu RD, Zhang X, et al. DsRNA-mediated silencing of Nudix hydrolase in *Trichinella spiralis* inhibits the larval invasion and survival in mice. *Exp Parasitol.* 2016; 162: 35–42. <https://doi.org/10.1016/j.exppara.2016.01.005> PMID: 26778819
61. Yang F, Yang DQ, Song YY, Guo KX, Li YL, Long SR, et al. In vitro silencing of a serine protease inhibitor suppresses *Trichinella spiralis* invasion, development, and fecundity. *Parasitol Res.* 2019; 118(7): 2247–55. <https://doi.org/10.1007/s00436-019-06344-4> PMID: 31081529
62. Liu RD, Wang ZQ, Wang L, Long SR, Ren HJ, Cui J. Analysis of differentially expressed genes of *Trichinella spiralis* larvae activated by bile and cultured with intestinal epithelial cells using real-time PCR. *Parasitol Res.* 2013; 112(12): 4113–20. <https://doi.org/10.1007/s00436-013-3602-1> PMID: 24026388
63. Yang DQ, Liu F, Bai Y, Zeng J, Hao HN, Yue X, et al. Functional characterization of a glutathione S-transferase in *Trichinella spiralis* invasion, development and reproduction. *Vet Parasitol.* 2021; 297: 109128. <https://doi.org/10.1016/j.vetpar.2020.109128> PMID: 32402492
64. Sun GG, Lei JJ, Ren HN, Zhang Y, Guo KX, Long SR, et al. Intranasal immunization with recombinant *Trichinella spiralis* serine protease elicits protective immunity in BALB/c mice. *Exp Parasitol.* 2019; 201: 1–10. <https://doi.org/10.1016/j.exppara.2019.04.006> PMID: 31004570
65. Guo X, Zhang H, Zheng X, Zhou Q, Yang Y, Chen X, et al. Structural and functional characterization of a novel gene, Hc-daf-22, from the strongylid nematode *Haemonchus contortus*. *Parasit Vectors.* 2016; 9(1): 422. <https://doi.org/10.1186/s13071-016-1704-1> PMID: 27472920
66. Haldar D, Sen D, Gayen K. Development of spectrophotometric method for the analysis of multi-component carbohydrate mixture of different moieties. *Appl Biochem Biotechnol.* 2017; 181(4): 1416–34. <https://doi.org/10.1007/s12010-016-2293-3> PMID: 27787768
67. Rao Ch S, Subash YE. The effect of chronic tobacco smoking and chewing on the lipid profile. *J Clin Diagn Res.* 2013; 7(1): 31–4. <https://doi.org/10.7860/JCDR/2012/5086.2663> PMID: 23449989
68. Gagliardo LF, McVay CS, Appleton JA. Molting, ecdysis, and reproduction of *Trichinella spiralis* are supported in vitro by intestinal epithelial cells. *Infect Immun.* 2002; 70(4): 1853–9. <https://doi.org/10.1128/IAI.70.4.1853-1859.2002> PMID: 11895947
69. Sun GG, Ren HN, Liu RD, Song YY, Qi X, Hu CX, et al. Molecular characterization of a putative serine protease from *Trichinella spiralis* and its elicited immune protection. *Vet Res.* 2018; 49(1): 59. <https://doi.org/10.1186/s13567-018-0555-5> PMID: 30001738
70. Liu P, Wang ZQ, Liu RD, Jiang P, Long SR, Liu LN, et al. Oral vaccination of mice with *Trichinella spiralis* nudix hydrolase DNA vaccine delivered by attenuated *Salmonella* elicited protective immunity. *Exp Parasitol.* 2015; 153: 29–38. <https://doi.org/10.1016/j.exppara.2015.02.008> PMID: 25733024
71. Ren HN, Liu RD, Song YY, Zhuo TX, Guo KX, Zhang Y, et al. Label-free quantitative proteomic analysis of molting-related proteins of *Trichinella spiralis* intestinal infective larvae. *Vet Res.* 2019; 50(1):70. <https://doi.org/10.1186/s13567-019-0689-0> PMID: 31547875
72. Yan SW, Hu YY, Song YY, Ren HN, Shen JM, Liu RD, et al. Characterization of a *Trichinella spiralis* cathepsin X and its promotion for the larval invasion of mouse intestinal epithelial cells. *Vet Parasitol.* 2021; 297: 109160. <https://doi.org/10.1016/j.vetpar.2020.109160> PMID: 32522393
73. Pozio E, Gomez Morales MA, Dupouy-Camet J. Clinical aspects, diagnosis and treatment of trichinellosis. *Expert Rev Anti Infect Ther.* 2003; 1(3): 471–82. <https://doi.org/10.1586/14787210.1.3.471> PMID: 15482143

74. Saad AE, Ashour DS, Abou Rayia DM, Bedeer AE. Carbonic anhydrase enzyme as a potential therapeutic target for experimental trichinellosis. *Parasitol Res.* 2016; 115(6): 2331–9. <https://doi.org/10.1007/s00436-016-4982-9> PMID: 26979731
75. Eid RK, Ashour DS, Essa EA, El Maghraby GM, Arafa MF. Chitosan coated nanostructured lipid carriers for enhanced in vivo efficacy of albendazole against *Trichinella spiralis*. *Carbohydr Polym.* 2020; 232: 115826. <https://doi.org/10.1016/j.carbpol.2019.115826> PMID: 31952620
76. Laskowska E, Kuczynska-Wisnik D, Lipinska B. Proteomic analysis of protein homeostasis and aggregation. *J Proteomics.* 2019; 198: 98–112. <https://doi.org/10.1016/j.jprot.2018.12.003> PMID: 30529741
77. Liu X, Song Y, Lu H, Tang B, Piao X, Hou N, et al. Transcriptome of small regulatory RNAs in the development of the zoonotic parasite *Trichinella spiralis*. *PLoS One.* 2011; 6(11): e26448. <https://doi.org/10.1371/journal.pone.0026448> PMID: 22096484
78. Janssen CS, Tetley L, Kennedy MW. Developmental activation of infective *Trichinella spiralis* larvae. *Parasitology.* 1998; 117 (4):363–71. <https://doi.org/10.1017/s003118209800314x> PMID: 9820858
79. Nowicki MW, Tulloch LB, Worrall L, McNae IW, Hannaert V, Michels PA, et al. Design, synthesis and trypanocidal activity of lead compounds based on inhibitors of parasite glycolysis. *Bioorg Med Chem.* 2008; 16(9): 5050–61. <https://doi.org/10.1016/j.bmc.2008.03.045> PMID: 18387804
80. Wang ZQ, Liu RD, Sun GG, Song YY, Jiang P, Zhang X, et al. Proteomic analysis of *Trichinella spiralis* adult worm excretory-secretory proteins recognized by sera of patients with early trichinellosis. *Front Microbiol.* 2017; 8: 986. <https://doi.org/10.3389/fmicb.2017.00986> PMID: 28620363
81. Hu CX, Jiang P, Yue X, Zeng J, Zhang XZ, Song YY, et al. Molecular characterization of a *Trichinella spiralis* elastase-1 and its potential as a diagnostic antigen for trichinellosis. *Parasit Vectors.* 2020; 13 (1): 97. <https://doi.org/10.1186/s13071-020-3981-y> PMID: 32093735
82. Maeda T, Saito T, Oguchi Y, Nakazawa M, Takeuchi T, Asai T. Expression and characterization of recombinant pyruvate kinase from *Toxoplasma gondii* tachyzoites. *Parasitol Res.* 2003; 89(4): 259–65. <https://doi.org/10.1007/s00436-002-0739-8> PMID: 12632162
83. Yang P, Ding GB, Liu W, Fu R, Sajid A, Li Z. Tannic acid directly targets pyruvate kinase isoenzyme M2 to attenuate colon cancer cell proliferation. *Food Funct.* 2018; 9(11): 5547–59. <https://doi.org/10.1039/c8fo01161c> PMID: 30259036
84. Ren HN, Zhuo TX, Bai SJ, Bai Y, Sun XY, Dan Liu R, et al. Proteomic analysis of hydrolytic proteases in excretory/secretory proteins from *Trichinella spiralis* intestinal infective larvae using zymography combined with shotgun LC-MS/MS approach. *Acta Trop.* 2021; 216: 105825. <https://doi.org/10.1016/j.actatropica.2021.105825> PMID: 33421420
85. Feng XM, Cao LJ, Wang FY, Zhang XC, Lu SQ. [Inhibition of pyruvate kinase mRNA expression in *Giardia lamblia* by specific hammerhead ribozyme]. *Zhongguo Ji Sheng Chong Xue Yu Ji Sheng Chong Bing Za Zhi.* 2010; 28(4): 257–60. PMID: 21137307